TURUN YLIOPISTON JULKAISUJA
ANNALES UNIVERSITATIS TURKUENSIS

SARJA - SER. D OSA - TOM. 810

MEDICA - ODONTOLOGICA

FIBER-REINFORCED COMPOSITE AS ORAL IMPLANT MATERIAL

Experimental studies of glass fiber and bioactive glass *in vitro* and *in vivo*

by

Ahmed Mansour Ballo

TURUN YLIOPISTO
Turku 2008

From the Department of Prosthetic Dentistry and Biomaterials Science, Institute of Dentistry, University of Turku, Turku, Finland.

Supervised by

Professor Timo Närhi
Department of Prosthetic Dentistry and Biomaterials Science
Institute of Dentistry
University of Turku
Turku, Finland.

and

Professor Pekka Vallittu
Department of Prosthetic Dentistry and Biomaterials Science
Institute of Dentistry
University of Turku
Turku, Finland.

Reviewed by

Docent Pekka Laine
Helsinki University Central Hospital
Helsinki, Finland

and

Professor Albert Feilzer
Department of Dental Materials Science
Academic Center for Dentistry Amsterdam (ACTA)
University of Amsterdam
Amsterdam, Netherlands

Dissertation opponent

Professor Flemming Isidor
Department of Prosthetic Dentistry
Faculty of Health Sciences, School of Dentistry
University of Aarhus
Aarhus, Denmark

ISBN 978-951-29-3630-4 (PRINT)
ISBN 978-951-29-3631-1 (PDF)
ISSN 0355-9483
Painosalama Oy – Turku, Finland 2008

In the name of Allah, the Most Merciful, the Most Kind.

To my Parents
&
my wife

TABLE OF CONTENTS

ABSTRACT

Ahmed Ballo

Fiber-reinforced composite as oral implant material: Experimental studies of glass fiber and bioactive glass *in vitro* and *in vivo*

Department of Prosthetic Dentistry and Biomaterials Science, Institute of Dentistry, University of Turku, Turku, Finland 2008.

Biocompatibility and mechanical properties are important variables that need to be determined when new materials are considered for medical implants. Special emphasis was placed on these characteristics in the present work, which aimed to investigate the potential of fiber-reinforced composite (FRC) material as an oral implant. Furthermore, the purpose of this study was to explore the effect of bioactive glass (BAG) on osseointegration of FRC implants.

The biocompatibility and mechanical properties of FRC implants were studied both *in vitro* and *in vivo*. The mechanical properties of the bulk FRC implant were tested with a cantilever bending test, torsional test and push-out test. The biocompatibility was first evaluated with osteoblast cells cultured on FRC substrates. Bone bonding was determined with the mechanical push-out test and histological as well as histomorplanimetric evaluation. Implant surface was characterized with SEM and EDS analysis.

The results of these studies showed that FRC implants can withstand the static load values comparably to titanium. Threaded FRC implants had significantly higher push-out strength than the threaded titanium implants.

Cell culture study revealed no cytotoxic effect of FRC materials on the osteoblast-like-cells. Addition of BAG particles enhanced cell proliferation and mineralization of the FRC substrates

The *in vivo* study showed that FRC implants can withstand static loading until failure without fracture. The results also suggest that the FRC implant is biocompatible in bone. The biological behavior of FRC was comparable to that of titanium after 4 and 12 weeks of implantation. Furthermore, addition of BAG to FRC implant increases peri-implant osteogenesis and bone maturation.

Keywords: Fiber-reinforced composite, bioactive glass, biocompatibility, oral implant, mechanical strength, osteoblast, osseointegration.

TIIVISTELMÄ

Ahmed Ballo

Kuitulujitteinen komposiitti implanttimateriaalina: Kokeellisia tutkimuksia lasikuidulla ja bioaktiivisella lasilla *in vitro* ja *in vivo*

Bioyhteensopivuus ja mekaaninen lujuus ovat tärkeitä ominaisuuksia, jotka tulee huomioida kun uusia materiaaleja harkitaan käytettäväksi lääketieteellisissä implanteissa. Näitä ominaisuuksia tutkittiin myös tässä työssä, jonka tavoitteena oli selvittää lasikuitulujitteisen komposiitin soveltuvuus hammasimplanttimateriaaliksi. Työn tarkoituksena oli lisäksi selvittää bioaktiivisen lasin vaikutus lasikuitulujitteisen implantin luuliitoksen muodotumiseen.

Lasikuitulujitteisen implantin mekaaniset ominaisuudet ja bioyhteensopivuus selvitettiin sekä *in vitro* että *in vivo* olosuhteissa. Lasikuitulujitteisen implantin mekaaninen kestävyys tutkittiin taivutus- ja kiertolujuus testeillä sekä ulostyöntökokeella (eng. push out test). Bioyhteensopivuus selvitettiin aluksi osteoblasteilla tehdyllä solukasvatus kokeella. Luuliitoksen muodostuminen tutkittiin biomekaanisella testillä sekä histologisen ja histoplanimetrisen tutkimuksen avulla. Implantin pinta karakterisoiin SEM ja EDS menetelmillä.

Tutkimustulokset osoittivat, että lasikuitulujitteinen implanttimateriaali kykenee vastustamaan staattista rasitusta titaanimateriaalin verrattavalla tavalla. Lasikuitulujitteisen ruuvi-implantin ulostyöntöä vastustava voima oli vastaavaa titaani-implanttia suurempi.

Lasikuitulujitteisilla materiaaleilla ei havaittu luusoluilla tehdyssä kokeessa solutoksisia vaikutuksia. Bioaktiivisen lasin lisääminen kuitulujitteisiin materiaaleihin edisti luusolujen kasvua ja solujen mineralisoitumista,

In vivo olosuhteissa tehty tutkimus osoitti, että lasikuitulujitteinen implantti kykenee vastustamaan ulostyöntä murtumatta luuliitoksen pettämiseen asti. Tämä työ osoitti myös, että lasikuitulujitteinen implantti on bioyhteensopiva luukudoksessa. Kuitulujitteisen implantin biologinen käyttäytyminen oli verrattavissa titaaniseen implanttiin 4 ja 12 viikon imlantointijaksojen aikana. Bioaktiivisen lasin lisääminen nopeutti lasikuitulujitteisen implantin luuliitoksen muodostumista ja implanttia ympäröivän luun maturoitumista.

Avainsanat: Kuitulijitteinen komposiitti, bioaktiivinen lasi, bioyhteensopivuus, hammasimplantti, mekaaninen lujuus, osteoblasti, osseointegraatio.

LIST OF ORIGINAL PUBLICATIONS

This thesis is based on the following original articles, which are referred to in the text by the Roman numerals I-V.

I. **Ballo AM, Lassila LV, Närhi TO, Vallittu PK.** *In vitro* mechanical testing of glass fiber-reinforced composite as dental implants. Journal of Contemporary Dental Practice. 2008; 9:41-8.

II. **Ballo AM, Lassila LV, Vallittu PK, Närhi TO.** Load bearing capacity of bone anchored fiber-reinforced composite device. Journal of Materials Science: Materials in Medicine. 2007; 18:2025-31.

III. **Ballo AM, Kokkari AK, Meretoja VV, Lassila LV, Vallittu PK. Närhi TO.** Osteoblast proliferation and maturation on bioactive fiber-reinforced composite surface. Journal of Materials Science: Materials in Medicine: accepted for publication.

IV. **Ballo AM, Akca E, Ozen T, Moritz N, Lassila LV, Vallittu PK, Närhi TO.** Bone bonding and bone formation of bioactive fiber-reinforced composite implants**.** Clinical Implant Dentistry and Related Research: submitted.

V. **Ballo AM, Akca E, Ozen T, Lassila LV, Vallittu PK, Närhi TO.** Bone tissue responses to glass fiber-reinforced composite implants – a histomorphometric study. Clinical Oral Implants Research: accepted for publication.

ABBREVIATIONS AND TERMINOLOGY

ANOVA: Analysis of variance
BAG: Bioactive glass
Bis-GMA: Bis-phenol-A-glycidyldimethacrylate
CT: Computer tomography
DC: Degree of conversion
EDS (=EDX, EDXA): Energy dispersive spectroscopy / X-ray analysis
FRC: Fiber-reinforced composite
FTIR: Fourier transform infrared spectrometry
HA: Hydroxyapatite
N: Newton
n: Number of specimens per group
PMMA: poly methyl methacrylate
S53P4: bioactive glass with silica content of 53 weight%
SEM: Scanning electron microscopy
TEGDMA: triethylenglycoldimethacrylate
(T_g): glass transition temperature
Wt%: Weight percentage

DEFINITIONS

Biocompatibility: A term used to describe the acceptance of a material as a biomaterial, that is, the material does not provoke rejection by the surrounding tissues and body as a whole. It is also the ability of a material to perform with an appropriate host response in a specific application.

Bioactivity: Spontaneous communication of a material in a biological environment resulting in strong adhesion between tissue and the material.

Bioinert: A material that retains its structure in the body after implantation and does not induce any immunological host reactions.

Biomaterial: Material intended to interface with biological systems to evaluate, treat, augment or replace any tissue, organ or function of the body.

Implant: Medical device made from one or more biomaterials intentionally placed within the body, either totally or partially buried beneath an epithelial surface.

Osteoconductivity: The ability of a structural scaffold to guide bone ingrowth.

Osseointegration: The direct structural and functional connection between living bone and the surface of a load-bearing artificial implant.

1. INTRODUCTION

In 1952, Professor Per-Ingvar Brånemark, a Swedish surgeon, while conducting research into the healing patterns of bone tissue, accidentally discovered that when pure titanium comes into direct contact with the living bone tissue, the two literally grow together to form a permanent biological adhesion. He named this phenomenon "*osseointegration*". With the introduction of osseointegration, the use of dental implants to support and retain dental prostheses had become predictable and offers the patient and the dentist an alternative treatment option.

Commercially pure titanium and its alloys are traditional materials used in most commercially available oral implants. The success of an oral implant is primarily based on good osseointegration, which depends on the biocompatibility of the implant material and implant surface properties, as well as on bone quantity and quality (Roynesdal *et al.*, 1998; Porter & Fraunhofer, 2005).

However, until now, none of the commercially available implants are able to attach to bone tissue with a periodontal ligament-like structure that might reduce the impact of the occlusal loads transmitted to the bone (Figure 1) (Misch *et al.*, 1999). In poor bone conditions, the mismatch of stiffness between bone and metallic implant may lead to implant failure (Lemons, 1998). This occurs when the tensile or compressive load exceeds the physiological limit of bone tolerance and causes microfracture at the bone-to-implant interface, or initiates bone resorption (Brunski, 1999).

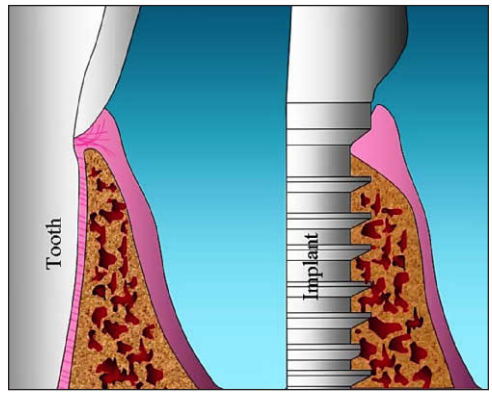

Figure 1. Schematic diagram of an endosseous dental implant and a tooth. Note that the implant lacks the periodontal ligament and is dependent on direct bone support (osseofixation).

Fiber-reinforced composites (FRC) are durable materials having lower elastic modulus than metals (Cheal *et al.*, 1992). In fact, the mechanical properties and modulus of

elasticity of unidirectional FRC (20-40 GPa) are close to that of natural bone (Goldberg & Burstone, 1992). There is growing interest in using FRCs in dental applications and surgical implants for orthopedic and craniofacial surgery involving some degree of structural performance under load-bearing conditions (Freilich *et al*., 2002; Behr *et al*. , 2001; Tuusa *et al*., 2007; Aho *et al*., 2004), which also makes FRCs interesting materials for oral implants (Figure 2).

Figure 2. One-piece design of threaded FRC implant.

Oral implants are exposed to complex loading conditions while functioning as anchors for prosthetic constructions. In addition to provide optimal conditions for a firm anchorage in bone tissue, the implant must also exhibit mechanical properties which will ensure a long-lasting function.

In principal, the one-piece design allows placement flexibility of the implant, as the final crown margin is prepared on the implant in a similar manner as for a natural tooth (Figure 3). With this design, the soft tissue is supported entirely by the implant body, irrespective of the shape of the osseous ridge.

Furthermore, the FRC implant is relatively easy to grind and modify directly in the mouth [in order] to properly restore the implant abutment area with composite superstructures without having the risk of overheating underlying bone.

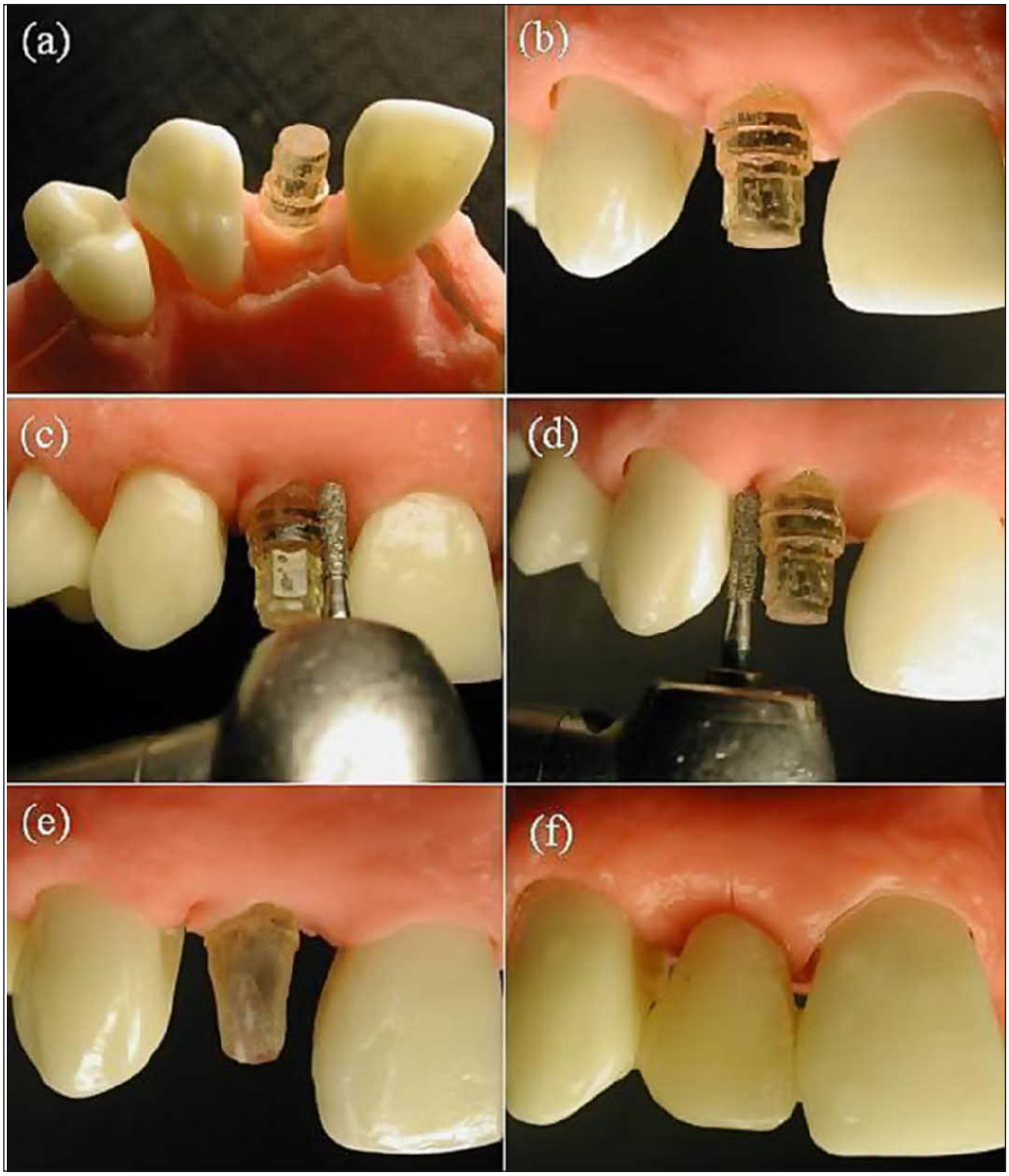

Figure 3. Clinical simulating illustration of placement and preparation of abutment portion of FRC implant.

2. REVIEW OF THE LITERATURE

2.1. Bone

Bone is a dynamic, vascular, living tissue that changes throughout life and is one of the so-called ‘‘connective tissues’’ of the body, thus comprising cells that become embedded in their own extracellular matrix (Bonucci, 2000). It has inorganic and organic parts. The inorganic is mainly crystalline mineral salts and calcium, which is present in the form of hydroxyapatite. The matrix is initially laid down as unmineralized osteoid which is manufactured by osteoblasts. Mineralization involves osteoblasts secreting vesicles containing alkaline phosphatase. This cleaves the phosphate groups and acts as the foci for calcium and phosphate deposition (Davies, 2000).

The organic part of the matrix is the mainly Type I collagen. This is made intracellularly as tropocollagen and then exported. It then associates into fibrils (Bevelander, 1971). The organic part of the matrix also includes various growth factors, the functions of which are not fully known. Other factors present include glycosaminoglycans, osteocalcin, osteonectin, bone sialoprotein and Cell Attachment Factor.

Bone can be either woven (coarse-fiber bone) or lamellar (layered). Woven bone is weak, with a small number of randomly oriented collagen fibers, but forms quickly and without a pre-existing structure during periods of repair or growth. Lamellar bone is stronger, formed of numerous stacked layers and filled with many collagen fibers parallel to other fibers in the same layer. After a break, woven bone quickly forms and is gradually replaced by slow-growing lamellar bone on pre-existing calcified hyaline cartilage through a process known as “bony substitution”.

Bone tissue is arranged in two macro-architectural forms: I) Trabecular (or cancellous, or spongy) and II) Cortical (or compact). These differences in macroarchitecture have been used to derive a clinical classification of bone type in the dental implant field, based on the relative proportion of cortical to trabecular bone (that is, where Class 1 bone is predominantly cortical as in the anterior mandible, while Class 4 bone is almost all trabecular as found in the posterior maxilla) (Leckholm & Zarb, 1985).

It has been observed that there is a relationship between bone structures and applied loads, this is referred to as Wolff’s law (Wolff, 1986). The bone acts as if it has some sensors that can measure the internal load and activate the bone cells to carry out the bone remodeling. Bone remodeling (Figure 4) appears to be governed by a feedback system in which the bone cells sense the state of strain in the bone matrix around them and either add or remove bone as needed to maintain the strain within normal limits.

This means that in order to preserve bone tissue, a dental implant should be designed so that it induces a mechanical stimulation in the surrounding bone, and high stress peaks do not arise in the bone.

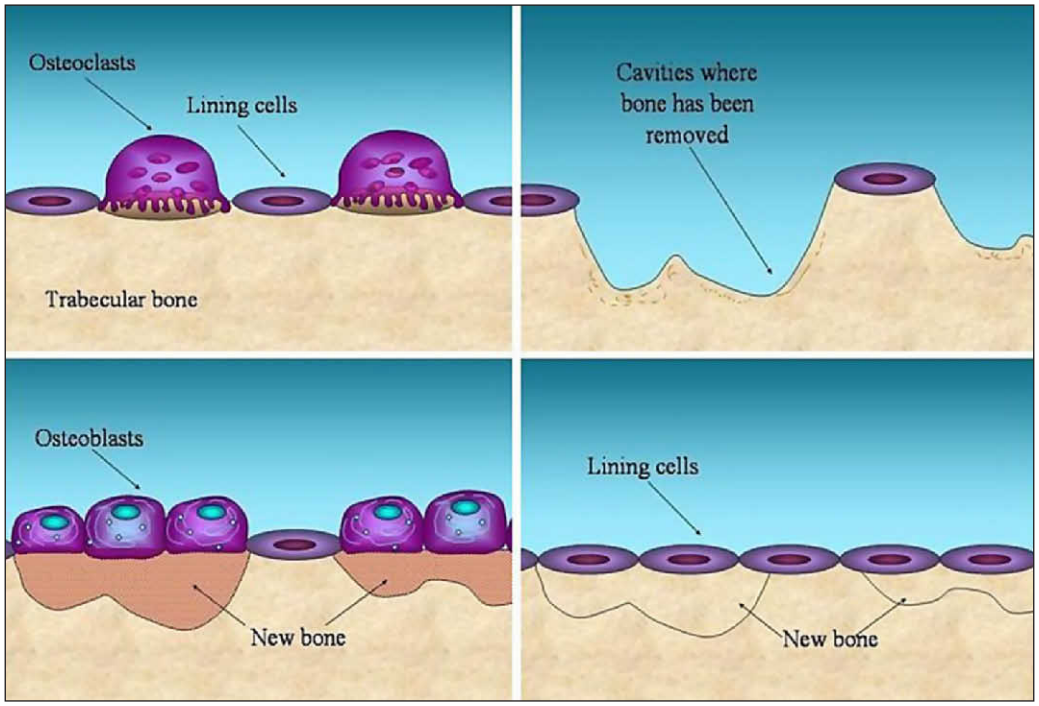

Figure 4. Schematic diagram illustrating bone remodeling process.

2.2. Osseointegration

Brånemark proposed that the titanium implant is structurally integrated into living bone with a very high degree of predictability without inflammation in soft and interface tissues or fixture rejection (Brånemark *et al.*, 1977). Brånemark placed his first Osseointegrated implant in a patient in 1965, after many years of pre-clinical studies.

The concept of osseointegration has thus significantly broadened from its original sense to its definition as a direct structural and functional connection between living alveolar bone and the dental implant as a load-carrier (Stanford & Keller, 1991).

The integration of an implant into bone has been widely studied in the literature and has long been considered a vital prerequisite for implant loading (Puleo & Nanci, 1999). Good primary stability is essential for achieving osseointegration (Brånemark *et al.*, 1977; Adell *et al.*, 1981; Meyer *et al.*, 2004). In fact, excessive mobility of the device may induce a fibrous membrane formation around the implant (Pilliar *et al.*, 1986; Soballe *et al.*, 1992).

During the clinical healing phase following placement, cellular attachment, migration and differentiation occur. Therefore, it is important to understand such fundamental characteristics as material selection, the physical and chemical properties of the implant surface which will affect the initial formation of host- tissue interface.

Peri-implant osteogenesis consists of woven bone and trabecular bone formation (Figure 5) which proceeds in two different directions: from the host bone towards the implant surface (distance osteogenesis) and from the implant surface toward the healing bone (contact osteogenesis) (Davies, 1998).

Figure 5. Histological view of bone formation pattern at blasted implant surface of titanium. (a) (Woven bone) 4 week of healing. (b) (Lamellar bone) 12 week of healing.

Once osseointegrated, the implants are connected to the prosthetic appliances and consequent bite forces are transmitted via the fixtures to the surrounding bone. The bone responds by initiating a continuous process during which it remodels itself into a state of balance around the implants.

Bone resorption is a major problem in implantation as it causes looseness at the bone-implant interface, thus undermining the integrity of the implant system (Huiskes *et al*., 1987). While stress-shielding (underload) is commonly regarded as a reason for bone resorption, high stresses (overload) at the interface have also been suggested as a contributing factor.

2.2.1. Implant failures

The high success rate of achieving osseointegration with screw-shaped endosseous implants is well documented (Adell *et al*., 1981; Branemark *et al*., 1985; Jemt &

Lekholm, 1993). Implant treatment failures, however, do occur, and what causes them is not always clear.

Implant failures could be divided into pre-osseointegration or post-osseointegration failures. Pre-osseointegration failure occurs when the implant fails to achieve integration with the surrounding bone and soft tissue. These failures to osseointegrate are most commonly related to placement of the implant into poor bone quality, hemorrhagic complications, and iatrogenic causes (O'Mahony & Spencer, 1999). Post-osseointegration failures are either biological or mechanical. Biological failures include periodontal infection (peri-implantitis), caused by poor oral hygiene, lack of attached gingival, or occlusal trauma caused by insufficient support for the forces that the implants are subjected to, such as weak bone, too few implants, poor prosthetic design, and parafunctional habits (Van Steenberghe *et al.*, 1999). Mechanical failure could be due to implant fracture, or to technical complications related to implant components and suprastructures (Berglundh *et al*., 2002; Pjetursson *et al*., 2004).

Considering the biomechanics of oral implants, both loading on the implant itself and the transferred load to the bone need attention. A key determinant of the success or failure of an oral implant treatment is the way mechanical stresses are transferred to the surrounding bone. Clinical (Quirynen *et al*., 1992; Naert *et al*., 1992; Baron *et al*., 2005) as well as experimental studies (Miyata *et al*., 2000, 2002) indicate that marginal bone loss at the oral implant may be associated with high occlusal stress on implants. The mismatch of stiffness between bone and metallic implant may lead to implant failure. This occurs when the tensile or compressive load exceeds the physiological limit of bone tolerance and causes microdamage at the bone-to-implant interface, replacing it with a soft tissue layer (Figure 6) (Isidor, 1996 & 1997).

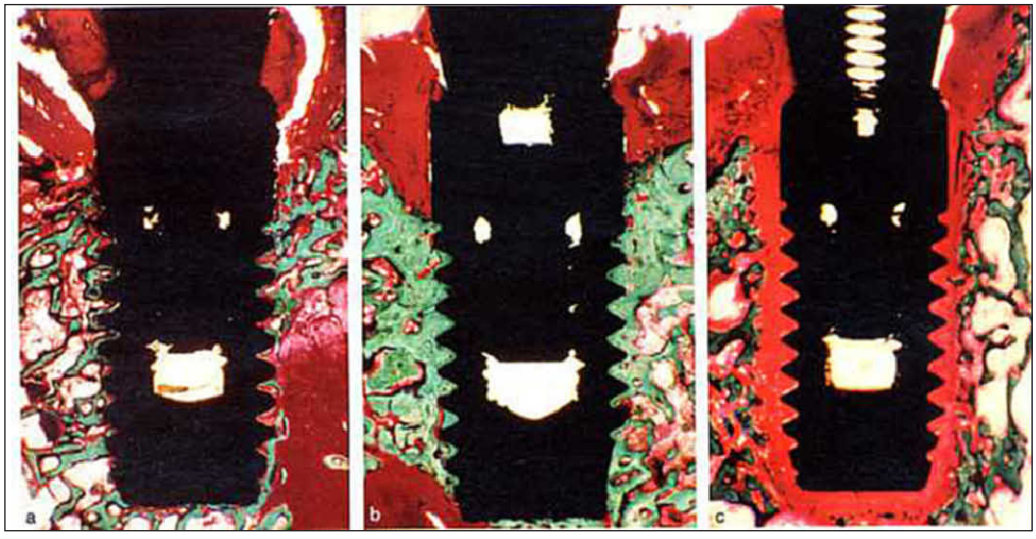

Figure 6. Histological section of a non-loaded implant (a) and two excessively loaded implants (b and c). The bone adjacent to the excessively loaded implant (c) could not adapt to load and the implant lost osseointegration completely. (Adapted from Clinical Oral Implant Research. 2006; 17:10)

2.3. Mechanical properties of implant biomaterials

Biomaterials are generally composed of a wide spectrum of materials. These implant biomaterials can be broadly classified into metallic, ceramic, polymeric, and composite materials.

An improperly chosen material can lead not only to failure of the part or a structure but also to unnecessary cost. Mechanical characterization is the classification of materials according to their mechanical properties. Table 1 illustrates some mechanical properties of these materials (O'Brien & William, 2002; Bouillaguet *et al*., 2006).

The main considerations in selecting metals and alloys for biomedical applications are biocompatibility, appropriate mechanical properties, and corrosion resistance. The high tensile and fatigue strength of metals, compared with ceramics and polymers, make them the materials of choice for implants that carry mechanical loads.

However, implants are made of metals that are stiffer than the bone which they contact. This leads to a large percentage of the load normally transmitted by the bone being borne by the prosthesis instead. This shielding can lead to bone disuse atrophy (Chrisman & Snook, 1968).

Table 1. Comparison of mechanical properties of different implant materials.

Property / Materials	Titanium	Alumina	Zirconia	Hydroxyapatite	FRC*
Strength (MPa)	800-1000	400-600	900-1200	115-150	700-1000
Young's modulus (GPa)	110-120	380	210	85	20-40
Hardness (HV)	100-140	2200	1200-1500	300-400	70-80

* Unidirectional fiber-reinforced.

Using an implant material which is biomechanically more suitable, which it is strong enough but also flexible so that it can reduce the interfacial stresses that causes fatigue fracture or resorption of the bone.

The flexibility or stiffness of a material may be described by the so-called modulus of elasticity (Young's modulus). The elastic modulus is the constant that relates the stress and the strain in the linear elastic region where elastic deformation of a material occurs (Figure 7) (Van Noort, 2002).

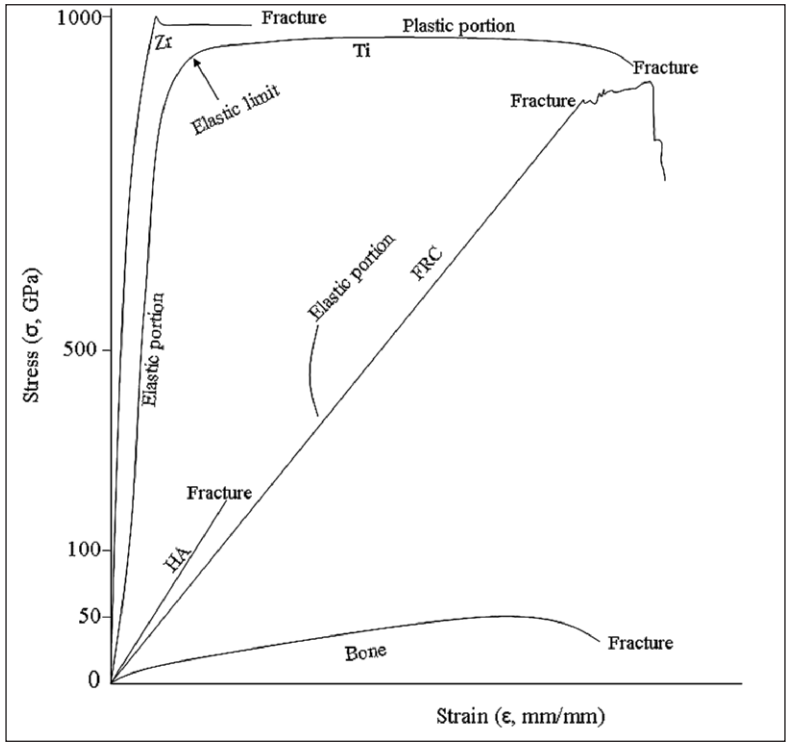

Figure 7. Average stress-strain curve for different materials.

Commercial-purity titanium (cp Ti) comes in a number of grades, with the mechanical properties being somewhat different for each grade. Small changes in the oxygen and iron contents greatly influence the mechanical properties, for example, Grade 3 cp Ti has Fe and O contents (maximum) of 0.3 and 0.35 %, respectively, and a yield strength of 380 MPa, while Grade 4 has Fe and O contents of 0.5 and 0.4%, respectively, and a yield strength of 483 MPa. The Ti-6%Al-4%V alloy, however, has a much higher value for yield strength (795 MPa), so this alloy is often chosen for dental implant cases where high strength is necessary (Mishra *et al.*, 1996). Compared with the elastic moduli of either stainless steel or cobalt-chromium, Ti and its alloys have much lower moduli that are still almost an order of magnitude higher than that of bone.

Ceramics are materials composed of metallic and nonmetallic elements held together by ionic and/or covalent bonds. Ceramic material has already been utilized as dental implant material like aluminum oxide (Al_2O_3) (Schulte, 1984). This material osseointegrated well but, unfortunately, the biomechanical properties of the implants were not sufficient for long-term load. As a result, this material was withdrawn from the market as dental implant material. Recently, Zirconia has been introduced as a new ceramic dental implant material. As a metal substitute, Zirconia possesses good chemical and physical properties, such as low corrosion potential and low thermal conductivity (Drouin & Cales, 1994; Piconi *et al*., 1998; Richter *et al*., 1994). Furthermore, its biocompatibility and biomechanical

properties as dental implant material have been extensively investigated (Albrektsson *et al*., 1985; Ichikawa *et al*., 1995; Kohal *et al*., 2006). However, these implant materials have very high elastic moduli compared to that of human bone (17–24 GPa).

Hydroxyapatite (HA) ceramics have been investigated extensively and used for dental implant applications for the past 30 years. The properties of HA depend on its porosity. Clinical studies have demonstrated that HA ceramics still remain the most biocompatible bone implant material known and possess the added feature of bonding strongly to living bone through natural-appearing bonding mechanisms (Chang *et al*., 1996), yet the range of problems include fractures during surgery and fractures after loading (Jarcho, 1992). Therefore, HA ceramics are not ideal materials for permanent implant devices. However, bioactive ceramic coatings on metal implants have kept ceramics as a key component in dental implantology (Krauser *et al*., 1990; Ogiso *et al*., 1996), although, delamination of the ceramic layer from the metal surface can create serious problems and lead to implant failure.

Polymers are widely used materials in biomedical applications. Polymers are used in drug delivery systems, and as a scaffolding material for tissue engineering applications. The polymeric materials have molecular structures completely different from living substances which make them generally more stable in the tissues.

Compared with metal and ceramics, polymers have much lower strength and moduli but they can be deformed to a greater extent before failure. Consequently, polymers are generally not used in biomedical applications that bear loads. Ultra-high-molecular-weight polyethylene is an exception, as it is used as a bearing surface in hip and knee replacements.

In high-load trauma applications such as bone fracture plates, screws and intramedullary nails, the strength of Polyetheretherketone (PEEK) polymer makes it a true alternative to metals (Kurtz & Devine, 2007), but polymerics are not yet commonly used for dental implants.

2.4. Implant surfaces

Biomaterials can also be roughly divided into three main types governed by the tissue response. In broad terms, biotolerant materials illicit no or minimal tissue response. Bioactive materials encourage bonding to surrounding tissue with, for example, new bone growth being stimulated. Degradable or resorbable materials are incorporated into the surrounding tissue, or may even dissolve completely over a period of time. Metals are typically inert, ceramics may be inert, active or resorbable, while polymers may be inert or resorbable. Because the interactions between cells and tissues with biomaterials at the tissue implant interface are almost exclusively surface phenomena, surface properties of implant materials are of great importance. The bulk of a biomaterial presents physical and chemical properties of the material that remain during the lifetime of the implant.

However, the composition of an implant surface can differ markedly from the bulk composition due to specific effects related to the manufacturing conditions, such as machining, blasting, etching, coatings and sterilization procedures.

Metallic implants are characterized by protective oxide layers resistant to corrosion, but ion release is still common with these materials (Jacobs *et al.*, 1998), and is a function of the passivation state, composition, and corrosion potential. Ti and its alloy have shown excellent inertness, and resistant to corrosion by body fluids and apparently compatible with living tissue (Branemark *et al.*, 1977; Adell *et al.*, 1981; Parr *et al.*, 1985), and thus combine many of the attributes desirable for an implant material.

An effective surface treatment for titanium appears to be passivation or anodization in a suitable solution prior to implantation (Steinemann, 1998). Because of this, the healing process is slower compared to other implant materials with bioactive properties such as bioglass (Hench, 1999) or hydroxyapatite (Lewis, 2000; Sun *et al*., 2001).

Implant surface modification including sandblasting, acid etching in combination with grit blasting (Cochran *et al*., 1998) and calcium phosphate coatings formed directly by plasma spraying (Klein *et al*., 1994), and wet chemical deposition (sol-gel) (Jansen *et al*., 1993) have been investigated as way to increase osteoconductivity (Figure 8). It has been proposed that increasing osteoconductivity by these surface design strategies is related to the altered implant topography that results from the surface modification arising from enhanced osteoblast and preosteoblast adhesion, thereby leading to accelerated bone formation (Chehroudi *et al*., 1992; Cooper *et al*., 1998).

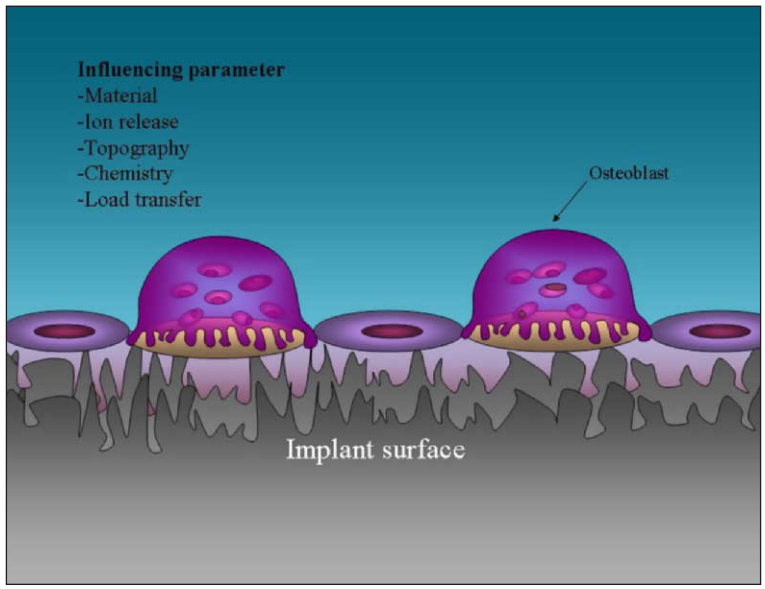

Figure 8. Influencing material surface parameter on osteoblast behavior.

There is a wide range of ceramic coatings containing calcium and phosphorus, with the primary difference in many of these materials being in the rate of ion release. Although their long-term success rate is unknown, the calcium phosphate surfaces seem to have a higher potential for attachment of osteoinductive agents than do uncoated titanium and other more inert implant materials (Maxian *et al*., 1993; Chang *et al*., 1999).

Minimal ion release has been noted for aluminum oxide or zirconium oxide under normal conditions. The ionic ceramic surface is in a high oxidation state, thermodynamically stable and hydrophilic, so water bonds to the surface with a relatively high strength of attachment (Heimke, 1990).

Polymers may contain various additives, traces of catalysts, inhibitors, and other chemical compounds needed for their synthesis. Over time in the physiological environment, these compounds can leach from the polymer surface. As is the case with corrosion by products released from metallic implants, the chemicals released from the polymers may induce adverse local and systemic host reactions that cause clinical complications. This release is of concern for materials, such as bone cement, that are polymerize in situ.

The use of acrylic implants was not a success due to problems with the material (van Mullem *et al*., 1988), including low strength, and release of the monomer into the surrounding tissue. These polymers are also hydrophobic and have little adhesion to living cells in spite of their high stability.

2.5. Fiber-reinforced composites (FRC)

FRC are a relatively new group of materials among those that have been investigated in dental or medical applications over the last 40 years (Smith, 1961). Their use is growing in many dental applications, including implant supported prostheses (Freilich *et al*., 2002; Behr *et al.*, 2001; Duncan *et al.*, 2000).

Composites are combination of two materials in which one of the materials, called the reinforcing phase, is in the form of fibers or particles, and is embedded in the other material called the matrix phase. The role of the reinforcement in a composite material is fundamentally one of increasing the mechanical properties of the neat resin system, while the resin combines the fibers together and protects the fibers from the external environment moisture (Vallittu, 1996).

All of the different fibers used in composites have different properties and so affect the properties of the composite in different ways. It is also necessary to specify the geometry of the reinforcement, its concentration, distribution and orientation (Alexander, 1996).

Glass-fiber reinforcements were produced for the first time in 1893. E-glass fiber takes its name from its electrical properties. Now it is one of the most attractive reinforcements

due to its high performance, good properties and low cost. It is made up of silicon oxide and some other oxide. Glass fibers are the most commonly used reinforcing fibers in both dental and industrial applications. They have several advantages such as high tensile strength, excellent compression and impact properties, relatively high E-modulus, resistances to high temperatures and corrosive environments, and also good esthetic appearance.

Fibers are mechanically more effective in achieving a durable and stiff composite than particulate fillers, and with the aid of fibers, the load-bearing capacity of the material can be increased. However, the loading and direction of the fibers influence the stiffness and strength of the composite.

Unidirectional fiber-reinforced composite has relative strength and stiffness comparable to metal when loading along the fibers, but with much less weight. Because of the anisotropic nature of unidirectional FRC, the material has different physical properties in different directions. So designing the FRC device should be done carefully.

Unidirectional fibers can most effectively reinforce the composite when positioned on the tension side (Dyer *et al.*, 2004). When the fiber content in the composite increases, the strength and modulus of elasticity of the composite also increase (Vallittu, 1998). Fibers can be oriented in two directions as woven fibers if the stiffness and strength are needed in several directions.

Effective wetting of fibers by the resin matrix, also called resin impregnation, is a prerequisite for their effective use (Vallittu, 1995 & 1998). With good impregnation, optimal reinforcement and transfer of stresses from the polymer matrix to reinforcing fibers may be achieved. An improper degree of impregnation causes increasing water sorption through voids, leading to reduced mechanical properties of FRC (Miettinen & Vallittu, 1997).

In the case of photopolymerization of FRC, the light intensity, exposure time and the polymerization temperature have an effect on flexural properties and monomer conversion (Loza-Herrero *et al.*, 1998).

Recently, attempts have been made to use FRC as implant material in craniofacial surgery (Tuusa *et al.*, 2007). However, there is a limited amount of scientific literature on using FRC material as surgical devices.

3. AIMS OF THE PRESENT STUDY

This study was based on the working hypothesis that fiber-reinforced material is biocompatible in bone environment and sufficiently durable as an oral implant under mechanical loading conditions. Another working hypothesis was that the addition of bioactive glass to fiber-reinforced composite will improve bone bonding of the FRC implant.

Consequently, the following specific aims were set to study the hypothesis:

1. To evaluate the design of fiber-reinforced composite on some mechanical properties (bending and torsion properties) of an oral implant (Study I).

2. To determine the load-bearing capacity of different FRC implant designs under push-out loading (Study II).

3. To evaluate the proliferation and maturation of osteoblast cells on different types of fiber-reinforced composite substrates (Study III).

4. To evaluate the interfacial strength between bone and fiber-reinforced composite implant with or without bioactive glass *in vivo* (Study IV).

5. To examine the bone response of inert and bioactive fiber-reinforced composite implants *in vivo* (Study V).

4. MATERIALS

The materials used for the fabrication of the test specimens and the implants in the current studies are listed in Table 2.

Table 2. The materials used for preparation of test specimens.

Product	Description	Manufacture	Lot no.	Composition	Study
Stick Resin	Light curing resin	Stick Tech, Turku, Finland	54031672	BisGMA-* TEGDMA**	I, II, III, IV and V
Ever Stick	Light-curing resin impregnated unidirectional fiber-reinforcement.	Stick Tech, Turku, Finland	2050426-ES-125	E-glass, PMMA***,Bis-GMA	I
Stick net fiber	Polymer preimpregnated bidirectional weave fiber	Stick Tech, Turku, Finland	2050523-W-0053	E-glass,**** PMMA	I, II, III, IV and V
E-glass fiber	Unidirectional fiber.	Ahlstrom, Karhula, Finland	11372313	E-glass	I, II, III, IV and V
BAG granules	(S53P4) granules size <45µm	Vivoxid Ltd Turku, Finland		SiO_2 53 wt%, Na_2O 23 wt%, CaO 20 wt% and P_2O_5 4 wt%.	II
BAG granules	(S53P4) granules size 90-315µm	Vivoxid Ltd Turku, Finland		SiO_2 53 wt%, Na_2O 23 wt%, CaO 20 wt% and P_2O_5 4 wt%.	II, III, IV and V

*Bis-GMA, bisphenol A-glycidyl dimethacrylate.
**TEGDMA, triethylenglycoldimethacrylate.
***PMMA, poly methyl methacrylate, Mw 220.000
**** E-glass, electrical glass

4.1. Resin systems

The resin system used to impregnate the FRC material in the studies is Stick Tech Ltd (Turku, Finland) produced the resin system (Stick® Resin) were dimethacrylate-monomethacrylate (BisGMA-PMMA) system that produced semi-interpenetrating polymer network to polymer matrix. The resin matrix contained 1 wt % of camphorquinone and DMAEMA (N,N-dimethyl aminoethyl methacrylate) as the photo-initiator.

4.2. Glass fibers

Continuous unidirectional silanized E-glass fiber and the bi-directional silanized E-glass weaves (Figure 9) were supplied by Stick Tech Ltd (Turku, Finland) in the form of resin-impregnated prepregs (everStick), polymer-preimpregnated fibers (StickNet), or as plain

glass fibers. The diameter of an individual fiber was 15 μm for unidirectional fibers and 6 μm for bi-directional weaves. One unidirectional bundle contained 4000 fibers. The composition of the E-glass fibers was SiO_2 55 wt%, CaO 22 wt%, Al_2O_3 15 wt%, B_2O_3 6 wt% and MgO 0.5 wt%. In addition, there were also minor amounts (less than 1.0 wt %) of other metal oxides (Fe, Na, K).

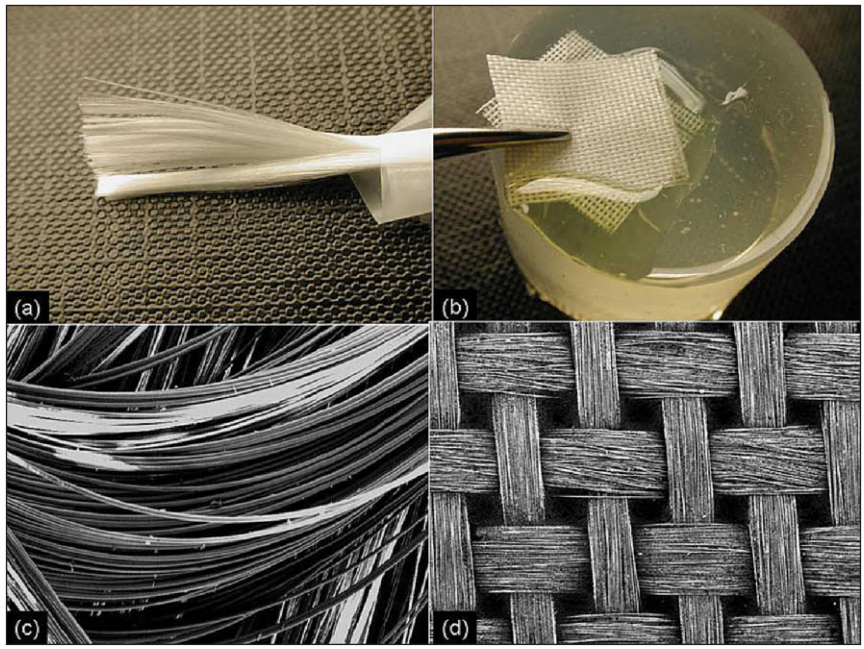

Figure 9. Unidirectional and bidirectional E-glass fibers and their features under SEM.

4.3. Bioactive glass

Vivoxid Ltd (Turku, Finland) produced the commercially available bioactive glass (S53P4) granules. Two different size BAG granules were used: a) <45μm and b) 90-315μm. The composition of BAG by weight is: SiO_2 53 wt%, Na_2O 23 wt%, CaO 20 wt% and P_2O_5 4 wt%.

5. METHODS

5.1. Test specimen and implant fabrication

The test specimens and implants were had same polymerization condition with differences in the specimen shape according to the test type.

5.1.1. Polymerization condition

The test specimens were polymerized with an Optilux 501 (Kerr-Have., I, USA) hand light-curing unit, in a light-curing oven at 60° C in a vacuum (Visio Beta Vario 3M/ESPE, Seefeld, Germany) for 15 minutes to eliminate the oxygen inhibition layer on resin, and then in a light curing oven at 80°C (LicuLite, Dentsply De Trey GmbH, Dreieich, Germany) for 1 hour. To optimize the degree of monomer conversion (DC %) the specimens were post-cured in an oven for 24 h at 120° C. After polymerization, the specimens were wet ground with 1200 grit (FEPA) silicon carbide grinding paper after which the diameter and length of the specimens were measured in three different areas [in order] to record the final dimensions of the specimens. The specimens were conditioned in air at room temperature for 2 days before mechanical testing.

Table 3. Classification of experimental FRC specimens used in this study according to the polymerization conditions.

Study	Group	Initial light polymerization time	light-curing oven in vacuum	Light-curing oven polymerization	postcuring time (120 °C)	Design of FRC structure
I	A	40 s				Unidirectional fiber, resin impregnated (everStick)
I	B	40 s		15 min		Unidirectional fiber, resin impregnated (everStick)
I	C	40 s		15 min	1 h	Unidirectional fiber, resin impregnated (everStick)
I	D	40 s		1 h	1 h	Unidirectional fiber, resin impregnated (everStick)
I, II, III, IV and V	E	40 s	15 min	1 h	24 h	Unidirectional fiber, resin impregnated (everStick) with bidirectional fiber weave (0.05 mm in thick) wrapped around
I	F	40 s		1 h	24 h	Unidirectional fiber

Note: EverStick was used in the fabrication of PMMA specimens in groups A, B, C, D and E, whereas in group F the reinforcement was done using continuous unidirectional E-glass with manual bisGMA-TEGDMA resin impregnation (Stick Resin, StickTech).

5.1.2. Test specimens and implant shape

5.1.2.1. Preparation of cylindrical-shaped specimens for mechanical tests (Study I).

Molds with an internal diameter of 4 mm and lengths of 20 mm and 30 mm were used to prepare the specimens. The fibers were inserted into the mold along the long axis of the specimens. For the cantilever bending test, 10 mm of each specimen of 4 mm diameter and 20 mm length was embedded from one end into the center of a 10 mm x 10 mm x 10 mm acrylic resin block. For the torsional force test, 10 mm of each cylindrical specimen of 4 mm diameter and 30 mm length was embedded from both ends into center of a 10 mm x 10 mm x 10 mm acrylic resin block.

Six groups of specimens were prepared: eight specimens were fabricated for each group. Various polymerization conditions were tested for optimizing the polymerization of the resin matrix. Experimental materials and polymerization conditions of the specimens are summarized in Table 3.

5.1.2.2. Preparation of screw-shaped implants (Study II, IV and V).

The specimens were combined with five fiber-reinforcement bundles each consisting of 4000 continuous unidirectional E-glass fibers. The fiber bundle was impregnated manually in light-polymerizable bisGMA-TEGDMA resin. The group with fiber-reinforced thread was manufactured by adding bidirectional weave around the threads. Porous PMMA-weave reinforcements (StickNet) were further impregnated for 24 h in light polymerizable resin to dissolve PMMA, and to form a semi-IPN polymer network in polymerization.

Molds with an internal diameter of 4.1 mm and length of 10 mm were used to prepare the implants. The fibers were inserted into the mold along the long axis of the specimens.

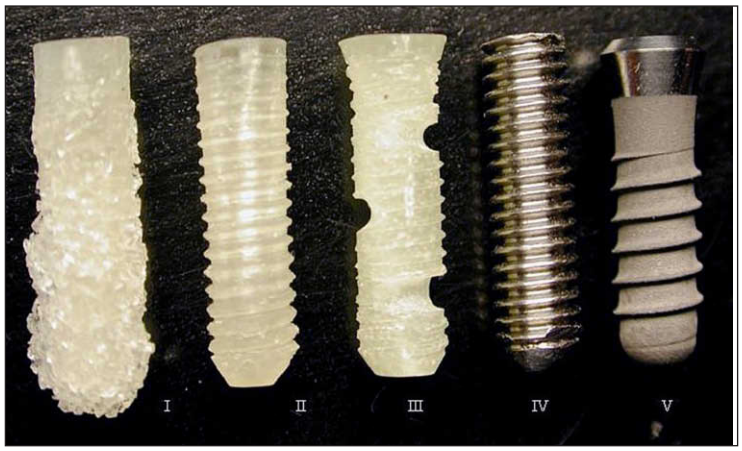

Figure 10. Picture of the experimental specimens for study II:
I. Non-threaded FRC device with bioactive glass coating.
II. Threaded FRC device.
III. Threaded BAG -coated FRC device with supplementary grooves.
IV. Custom-made titanium screw-shaped device.
V. Commercial Straumann dental implant.

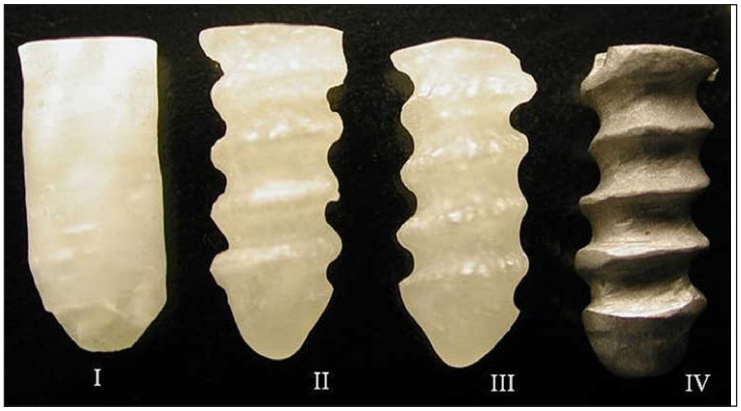

Figure 11. Picture of the experimental implants for studies IV and V:
I. Unthreaded FRC device with bioactive glass coating (IV).
II. Threaded FRC device (IV & V).
III. Threaded BAG-coated FRC device with supplementary grooves (IV & V).
IV. Custom-made titanium screw-shaped device (V).

5.1.2.3. Preparation of plate-shaped specimens for cell culture experiments (Study III).

The specimens, classified into the four following groups, were sterilized by autoclaving at 120°C for 20 min:

1. Blasted FRC (FRC group).
2. Blasted FRC with bidirectional fiber weave on the surface (FRC-Net group).
3. Blasted FRC with BAG coating (FRC-BAG group).
4. Blasted commercially pure (grade 2) titanium (cpTi) (control group).

5.2. Mechanical testing (I & II)

5.2.1. Bending and torsional tests (I)

The cantilever bending test was performed to measure the flexural properties of the specimens. A jig was used to provide a 45-degree angle between the long axis of the implant and the direction of the loading force (Figure 12). The specimens were loaded to failure by the Lloyd material testing machine (model LRX, Lloyd Instruments Ltd., Fareham, England) with a cross-head speed of 1.0 mm/min until fracture. Fracture force was determined as an audible crack or 10% reduction in force indicated by the testing device. The peak force of the failure of each specimen was recorded with PC software (Nexygen, Lloyd Instruments Ltd.). For the torsional force test, specimens were tested for the resistance of torsional force to failure using the universal Lloyd testing machine (model LRX, Lloyd Instruments Ltd., Fareham, England) with an angle speed of 16.2 degrees/min. The torsion sensor (TP-2KMCB Type, KYOWA machine Ltd., Tokyo, Japan) was used to measure the maximum torsional force of the specimen.

Figure 12. Cantilever bending test of the specimen.

5.2.2. Load-bearing capacity of threaded FRC (II)

The specimens were embedded into gypsum plaster using the powder-liquid ratio of 100 g / 20 ml as recommended by the manufacturer. The gypsum/specimen blocks were fixed in the testing device and loaded by downwards vertical force with the Lloyd material testing machine (model LRX, Lloyd Instruments Ltd., Fareham, England) with cross-head speed of 1.0 mm/min until failure of the specimen-gypsum interface (Figure 13). The peak force of failure was recorded with PC computer Software (Nexygen, Lloyd Instruments Ltd.).

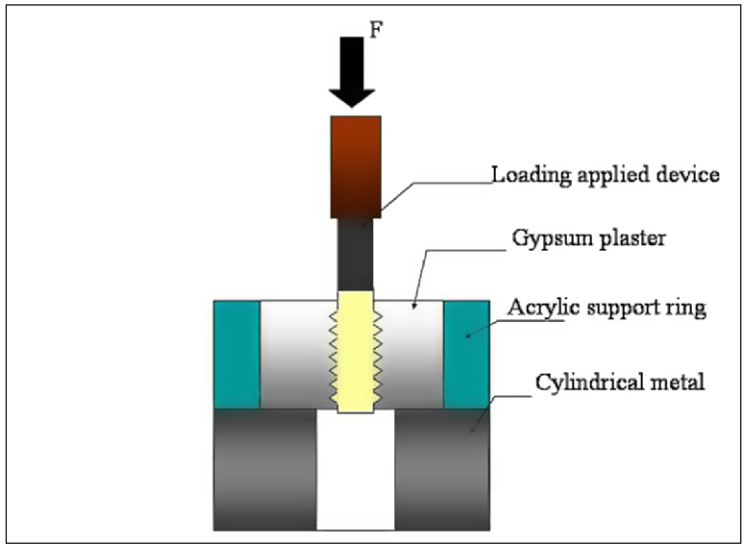

Figure 13. Push-out test of the specimen.

5.3. FTIR spectroscopy (I)

In study I, The degree of monomer conversion (DC %) of the polymer matrix of mechanically tested specimens after various polymerization modes was monitored by Fourier transform infrared spectroscopy (FTIR) (Spectrum one, Perkin Elmer, Beaconsfield Bucks, UK) with an attenuated total reflectance (ATR) sampling accessory. The mechanically tested specimens were ground by grinding stone to receive the powder to be placed on the surface of the detector ZnSe-ATR crystal. The spectrum of unpolymerized resin matrix of everStick reinforcement (Stick Tech Ltd, Turku, Finland) was used to measure the DC% of polymer powder of each specimen. Each spectra was recorded with 16 scans using a resolution of 4 cm. The DC% was calculated from the aliphatic C=C peak at 1638 cm^{-1}, and normalized against the aromatic C=C peak at 1608 cm^{-1} according to the formula.

$$DC\ \% = \left[1 - \frac{C_{aliphatic} / C_{aromatic}}{U_{aliphatic} / U_{aromatic}}\right] \bullet 100\%$$

Where:

$C_{aliphatic}$ = absorption peak at 1638 cm^{-1} of the cured specimen.

$C_{aromatic}$ = absorption peak at 1608 cm^{-1} of the cured specimen.

$U_{aliphatic}$ = absorption peak at 1638 cm^{-1} of the uncured specimen.

$U_{aromatic}$ =absorption peak at 1608 cm^{-1} of the uncured specimen.

5.4. Cell culture experiments (III)

5.4.1. Cell cultures

Rat bone marrow stromal cells were harvested and cultured according to Maniatopoulos *et al.* (Maniatopoulos *et al.* 1988). Briefly, femurs were isolated from two six-week old male Sprague-Dawley rats. The bones were wiped with 70% alcohol and immersed twice in α-MEM (Sigma chemical Co., USA) culture medium containing 100 units/ml of penicillin/ streptomycin (Gibco BRL, Life Technologies BV, The Netherlands). The condyles were cut off, and the bone marrow was flushed out using complete cell culture medium (α-MEM with 15 % fetal bovine serum (Gibco) and supplemented with 50 µg/ml ascorbic acid (Sigma), 7 mM Na-ß-glycerophosphate (Merck, Germany), and 10 nM dexamethasone (Sigma). The resulting suspension was passed through a 22 gauge needle. The adherent cell population was cultured in a humidified 5% CO_2 atmosphere at 37°C.

After seven days of primary culture, cells were trypsinized and resuspended in complete culture medium. Cell culture substrates were placed into non-treated 24-well plates (Corning, USA) and washed with phosphate-buffered saline (PBS) for one hour, and with complete cell culture medium for three hours at 37°C. Cell suspension was subsequently

added to the test substrates at a density of 20 000 cells / cm^2 and allowed to adhere overnight. After seeding, osteoblast culture was continued for three weeks with medium replacement every 2 to 3 days.

Cells seeded on conventional tissue culture polystyrene wells at a density of 10 000 cells / cm^2 were used as a positive cell control. The cells expanded to confluence, and exhibited typical osteogenic phenotype, starting to mineralize after 14 days of culture.

5.4.2. Ion concentration analysis

Silica and calcium concentrations in the used cell culture medium were analyzed from four to six replicate culture wells before each medium change. Three parallel measurements were carried out from each medium sample.

Colorimetric measurement of silica concentration was based on the molybdenum blue method (Fanning & Pilson, 1973). The Silicomolybdate complex was reduced with a mixture of 1-amino-2-naphthol-4-sulphonic acid and sulphite, and tartaric acid was used to eliminate interference from phosphate. Calcium concentrations were determined using the ortho-cresolphtalein complexone (OCPC) method (Lorentz, 1982). The assay reagent consisted of OCPC with 8-hydroxyquinol in an ethanolamine/boric acid buffer. Absorbances (820 nm for silica and 560 nm for calcium) were measured using either a UV-1601 spectrophotometer (Shimadzu, Australia) or a Multiskan MS ELISA plate reader (Labsystems, Finland).

5.4.3. Proliferation assay

The amounts of cultured cells were determined using AlamarBlue™ (AB) assay (BioSource International, USA) in colorimetric format. At predetermined times, specimens (n=4) were withdrawn from the culture, and placed into clean 24-wells. Fresh assay solution (phenol red-free DMEM with 10 % serum and including 10 % AB reagent) was added to the wells. After three hours' incubation, absorbance values of the solution were taken at 560 nm and 595 nm using the ELISA plate reader. The measured absorbances were used to calculate the reduction of the AB reagent in accordance with the manufacturer's instructions. Reductive cell activity of cultured osteoblasts has been shown to correlate with their numbers (Jonsson *et al*., 1997). The cell activities were normalized in relation to the activity of the titanium control at the first time point.

5.4.4. Alkaline phosphatase activity

At predetermined times, four replicate specimens were washed with phosphate-buffered saline (PBS) and placed into clean 24-wells containing 750 µl lysis buffer (25 mM HEPES, 0.1 % Triton X-100, 0.9 % NaCl, pH 7.6). The immersed specimens were stored at -70°C until the amounts of total protein and alkaline phosphatase (ALP) activity were measured from supernatants diluted with 0.9 % NaCl as needed.

Amounts of total protein were measured with a Micro BCA™ protein assay reagent kit (Pierce, USA) according to the manufacture's microwell plate protocol. Briefly, equal amounts of supernatant and working reagent were combined and incubated at 37°C for two hours. Mean readings of absorbances from three replicate wells were recorded at 560 nm, using the ELISA plate reader. Protein concentrations were read from a bovine albumin (Pierce) standard curve.

To measure ALP activity, 50 µl of supernatant and 200 µl of para-nitrophenyl phosphate substrate solution (Sigma) were combined on a microwell plate. The plate was incubated at 37°C for one hour, and 50 µl of 3 M NaOH solution was added to each well to stop the enzymatic reaction. Mean readings of absorbance from three replicate wells were recorded at 405 nm, using the ELISA plate reader. Amounts of converted substrate were read from a para-nitrophenol standard curve. Measured ALP activities were normalized in relation to the amounts of protein determined.

5.4.5. RT-PCR

At predetermined times, total cellular RNA from culture substrates was isolated using Trizol® reagent (Gibco). Four replicates from each substrate type were reverse transcribed with random hexamer primers using a GeneAmp Gold RNA PCR Reagent kit (Applied Biosystems, USA). The resultant first-strand cDNA was analyzed in duplicate PCR reactions using FAM-labeled TaqMan® Gene Expression Assays (Applied Biosystems) for bone sialoprotein (BSP; Rn00561414_m1), osteocalcin (OC; Rn00566386_g1) and glyceraldehyde-3-phosphate dehydrogenase (GAPDH, a control gene; Rn99999916_s1). PCRs were carried out using an iCycler iQ real-time PCR detection system with software version 3.1 (Bio-Rad Laboratories). The following cycling conditions were used: 95°C / 5min; 40 cycles of 95°C / 20s, and 60°C/ 60s. The threshold cycles (C_T) were automatically calculated using ''the maximum curvature approach'' and gene expression levels of BSP and OC were normalized to GAPDH expression in each RNA sample ($\Delta C_T = C_{T,\,target} - C_{T,\,GAPDH}$). A difference of one unit in ΔC_T value corresponds to a two fold difference in gene expression level.

5.5. Animal experiments (IV and V)

Six female pigs, 14 to 16 months old, with an average body weight of 60 kg were used in this study. A total of 24 implants were placed into the right and left tibia of each experimental animal (Figure 14). This study was approved by the Animal Ethics Committee of the University of Gulhane Medical Academy, Ankara, Turkey, under the reference number 10/04/2006 Ethics-2006-27. All national guidelines for the care and use of laboratory animals were followed.

5.5.1. Surgical procedure

All surgery was performed under sterile conditions in a veterinary operating theatre. The animals were sedated with an intramuscular injection of ketamine (10 mg/kg, Fort Dodge Laboratories, Fort Dodge, IA, USA), atropine (0.06 ml/kg, Elkin-Sinn, Cherry Hill, NJ, USA) and stresnil (0.03 ml/kg, Janssen Pharmaceutica, Beerse, Belgium). The tibias were exposed by skin incisions and via fascial-periosteal flaps. The experimental implants were placed with the press-fit technique (implant bed diameter equals the diameter of implant) using the same drills for all implant beds. The drilling was done under continuous external sterile saline irrigation to prevent from overheating the bone. The implants were placed randomly in the tibia according to a previously designed arrangement. The implant sites were sequentially enlarged following the standard protocol of traditional dental implant placement.

After placing the implants, the skin and the fascia-periosteum were closed in separate layers with single resorbable sutures. Prophylactic antibiotic was administered subcutaneously (benzylpenicillin/dihydrostreptomycin, Tardomycel, BayerVital, Germany), 2.5 ml every 48 h for 7 days.

The animals were inspected during the first days after surgery for signs of wound dehiscence or infection and weekly thereafter to assess their general health.

Three animals were euthanized after a 4-week, and three animals after a 12-week healing period with an overdose intravenous injection of Pentobarbital® (Pentotal R sodium, Abbott Lab. S.A., Spain). Tibia blocks containing the implants and surrounding tissues were dissected from all animals. The blocks were sectioned with a bandsaw and processed for the mechanical testing.

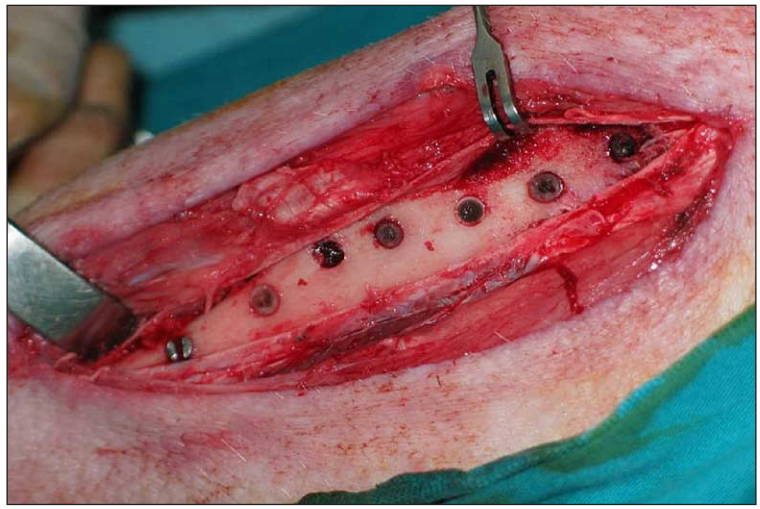

Figure 14. Photograph of surgical procedure after placement of experimental implants in the tibia of a pig.

5.6. Micro-CT analysis (IV)

The implant/bone blocks were imaged by micro-computer tomography (Skyscan 1072 micro-CT, Skyscan n.v. Aartselaar, Belgium). The angle of 180 degrees and the step angle of 0.9 degrees were used, with resolution of 2 μm per pixel. The interface between the implant and the periimplant bone was examined using CT-Analyzer version 1.5.0.0 software (Skyscan n.v. Aartselaar, Belgium) Because of the low contrast differences between bone and implant, the volumetric analysis was performed in two stages. The volume of the implant was measured using a manually defined volume of interest (VOI) that followed the shape of the implant; then the combined volume of the implant and the peri-implant bone was measured using a second manually defined VOI that contained bone between the threads (TV: mm^3). The subtraction of the two VOIs produced the quantitative estimate of the bone between the threads (BV: mm^3): the relative bone volume (BV/TV: %).

5.7. Determination of bone bonding strength (IV)

The bone block was fixed in a cylindrical support using a self-curing acrylic resin. During the cement hardening the bone specimens were kept in place using the fixture axis as a reference. The cylinders were fixed in the testing device and loaded by downwards vertical force with a Lloyd mechanical testing machine (model LRX, Lloyd Instruments Ltd., Fareham, England) at a cross-head speed of 1.0 mm/min until failure (Figure 4 in original publications). The peak force of failure was recorded with PC computer Software (Nexygen, Lloyd Instruments Ltd.).

5.8. Scanning electron microscopy, SEM (I, II, III, IV and V)

A scanning electron microscope (SEM) (JSM 5500, Jeol Ltd, Tokyo, Japan) was used for visual microscopic examination of fracture surfaces in the different specimens and implant type after loading, in studies I, II and IV. After the cantilever bending test (Study I), all the specimens from each group were gold-sputtered (SCD 050, BAL-TEC AG, Balzers, Liechtenstein), and transverse section of the tested specimens were examined with SEM to determine the failure types and differences in test specimens after the bending test. In study II, after the push-out test, all the implant-shaped specimens that had been pushed out from the gypsum plaster disc were sputtered with gold and examined with SEM to evaluate the load-bearing capacity of the threaded FRC devices, and also to analyze the attachment of the BAG granules to the FRC device surface. In study IV, after the push-out test, all the implants that had been pushed out from the bone were dehydrated by 40 % ethanol for 24 h, by 70 % ethanol for 1 week, and embedded in acrylic resin. Samples were sectioned into two longitudinal sections and sputter-coated with carbon to analyze the failures between or within the different interfaces of the implant, the BAG and the bone, after testing.

In study III, the progression of osteoblast cultures was examined using SEM. Cell culture substrates were washed in PBS and fixed with 2 % glutardialdehyde in a 100 mM cacodylic acid buffer (pH 7.4). The fixed specimens were rinsed in buffer and either dried in a rising alcohol series or stored in 70 % ethanol for subsequent SEM analysis. Dried specimens were carbon-coated before SEM imaging.

In study V, SEM/EDS analysis was performed for two samples [in order] to demonstrate the reactive layers of bioactive glass granules after implantation, as well as to find differences between the implant and surrounding tissues. SEM (Model JSM 5500, Jeol Ltd, Tokyo, Japan) and energy dispersive X-ray spectroscopy (EDS) analyses (Spirit, Princeton Gamma-Tech Inc., Princeton, NJ, USA) were carried out on the ground surfaces of test specimens after they had been dried in a desiccator and coated with a carbon layer. SEM micrographs and EDS analysis were carried out using a standardless method with an accelerating voltage of 20 KV, at a working distance of 20 mm.

5.9. Histological and histomorphometry analysis (V)

After 4 weeks and 12 weeks animals were sacrificed (3 pigs each time). Following euthanasia, tibia block specimens containing the implants and surrounding tissues were dissected from all of the animals. The block samples were sectioned with a saw to remove unnecessary portions of bone and soft tissue. The specimens were fixed and dehydrated in an ascending ethanol series and embedded in resin (Technovit 7200 VLC, Heraeus-Külzer). Undecalcified sections (80 μm) were prepared by the cutting and grinding method, and stained (hematoxylin and eosin) for routine light microscopic and computer-aided histomorphometric analysis using Leica Qwin v3.0 software (Leica Microsystems Imaging Solutions).

The histological evaluation consisted of examination of the tissue implant interface and the presence of inflammatory reaction. A grading scale was not used; the evaluation was based on isolated observations.

Images were captured using a stereo light microscope (magnification 6.53) with a digital camera (Leica DC300) connected to a personal computer (PC). Computer-assisted histoplanimetric analyses were performed with PC image analysis software (Leica Qwin v3.00). The amount of new bone formation on the implant surface was measured as an area % of the cross-section.

5.10. Statistical analysis

Statistical analyses were performed with SPSS (SPSS Inc, Chicago, Ill, USA) software for windows. The studied test groups (studies I, III, IV, V) were compared by one-way

or two-way ANOVA, followed by Tukey's post hoc analysis using a significance level of $p<0.05$.

In study II, push-out load values for all groups were analyzed with analysis of variance (ANOVA) (SPSS 11.0, SPSS Inc., Chicago, Ill, USA), followed by Tukey's post hoc analysis using a significance level of $p<0.05$. In addition, to evaluate the reliability of devices, Weibull analysis was carried using Weibull++ software (Reliasoft Corporation, Tucson, AR USA) according to the following formula:

$$P_f = 1 - \exp\left\{-\left(\frac{s - s_u}{s_o}\right)^m\right\}$$

Where m=Weibull modulus, s_o =characteristic push-out load and s_u = theoretical failure load (=0).

6. RESULTS

6.1. Mechanical test (I &II)

6.1.1. Bending and torsional tests

In study I, the maximum fracture load of the test specimens was evaluated. Tables 3 and 4 illustrate the mean fracture load values and standard deviations for the specimens. ANOVA revealed that post-curing significantly affected the fracture load ($p<0.001$). The mean fracture load values were: 437 N for group A, 581 N for group B, 961 N for group C, 1108 N for group D, 1461 N for group E, and 1200 N for group F. The torque could not be determined for the specimens in groups A, B, C and D, because of delamination of FRC prepregs in the early stage of loading. The mean torque was 1.66 Nm (range 1.3 to 1.9 Nm) for group E, and 1.0 Nm (range 0.8 to 1.4 Nm) for group F.

Table 4. The mean failure load values and standard deviation of the test specimens in cantilever bending test (n=8). Same superscript letter indicates that groups did not differ statistically significantly ($p<0.05$).

Group	Failure load (N)	Standard deviation
A	437 [a]	64
B	581 [b]	97
C	961 [c]	186
D	1108 [c]	170
E	1461 [e]	112
F	1200 [d]	109

Table 5. The mean maximal torque and standard deviation of the test specimens. (n=8) Same superscript letter indicates that groups did not differ statistically significantly ($p<0.05$).

Group	Maximum torque	Standard deviation
A	0.01 [a]	0.01
B	0.01 [a]	0.01
C	0.01 [a]	0.01
D	0.01 [a]	0.01
E	1.66 [c]	0.30
F	1.00 [b]	0.20

A= 40s initial light polymerization.
B= 40s initial light polymerization and 15 min light-curing oven polymerization.
C= 40s, 15 min light-curing polymerization and 1 h post-curing.
D= 40s, 1 h light-curing polymerization and 1 h post-curing.
E= 40s, 1 h light-curing polymerization and 24 h post-curing. (Unidirectional& bidirectional fiber).
F= 40s, 1 h light-curing polymerization and 24 h post-curing. (Unidirectional fiber).

6.1.2. Load-bearing capacity of threaded FRC (II)

Results of the push-out test are shown in Figure 15. The push-out force of Group IV (experimentally threaded titanium) was 778N (141N), which did not differ statistically ($p>0.05$) from the push-out force of Group I (unthreaded BAG-coated) 895 (122) N. However, 70% of the BAG coating was lost during the test. The push-out force of Group II (threaded FRC) was 1277 (137) N, which was statistically ($p>0.05$) similar to the force of Group V (Straumann SLA implant) 1395 (183) N.

The highest push-out forces, 2302 (265) N, were recorded for Group III (threaded FRC/BAG specimens with supplementary grooves). In all FRC devices, the screw threads could retain the push-out load and no thread failures were observed.

Weibull analysis revealed the lowest Weibull modulus 5.95, and a characteristic push-out force of 836 N for Group IV (experimental titanium), which reveals the lowest reliability within the studied groups. The Weibull modulus of FRC devices varied between 7.75 and 11.94, which suggests improved reliability (Figure 7 in original publication). Figure 16, illustrates the fracture surface of the polymeric threaded FRC device after the push-out test.

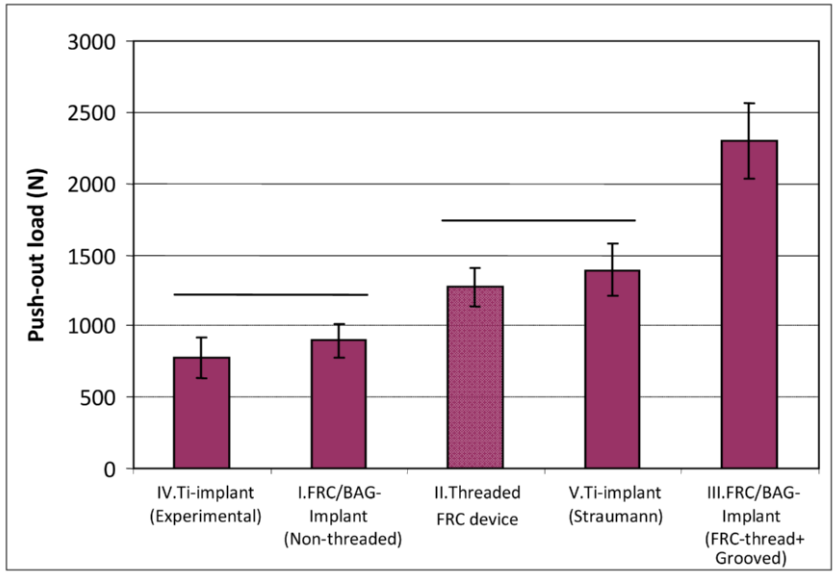

Figure 15. Results of mean values of push-out test. Horizontal line above bars represents homogeneous subsets (Tukey post hoc test).

Figure 16. SEM micrograph of fracture surface of polymeric-threaded FRC device after push-out test. Fracture occurred through outer layer of FRC threads, suggesting that main failure reason was low cohesive shear strength of plaster.

6.2. Determination of degree of conversion (I)

Degree of monomer conversion (DC %) is presented in Table 6. The mean DC% was increased in all groups by increasing the time of light-curing and by increasing the post-curing temperature. The specimens in group A had the lowest DC%: the mean DC% was 53% for group A, 61% for group B, 73% for group C, 75% for group D and 90% for groups E and F.

Table 6. The degree of conversion (DC %) and standard deviation of polymer matrix of tested specimens after different polymerization conditions. Same superscript letter indicates that groups did not differ statistically significantly ($p<0.05$).

Group	DC%	standard deviation
A	53.1 [a]	3.1
B	61.3 [b]	2.7
C	73.4 [c]	1.2
D	75.0 [c]	0.8
E & F	89.8 [d]	1.9

6.3. Cell culture experiments (III)

6.3.1. Ion concentration analysis

Dissolution of BAG from FRC-BAG specimens released alkali ions and soluble silica into the cell culture medium. Leached alkali increased culture pH by 0.1-0.2 units when compared to other materials (data not shown). Furthermore, high concentrations of calcium and silica were initially observed (Figure 17). Cells on FRC-BAG substrates started to mineralize by day 9, as indicated by depletion of calcium from the culture medium. Calcium concentrations in the used culture mediums were significantly lower ($p < 0.05$) than those in medium blanks from day 9 onwards. However, on days 9 and 11, there was calcium precipitation on only four out of six analyzed FRC-BAG substrates. By day 14, all the replicate specimens had started to mineralize. Calcium depletion on FRC and FRC-Net did not take place until day 21 in culture. At that time, precipitation was observed on all FRC, but only on half of the FRC-Net replicas. No calcium precipitation was observed on titanium substrates at any time.

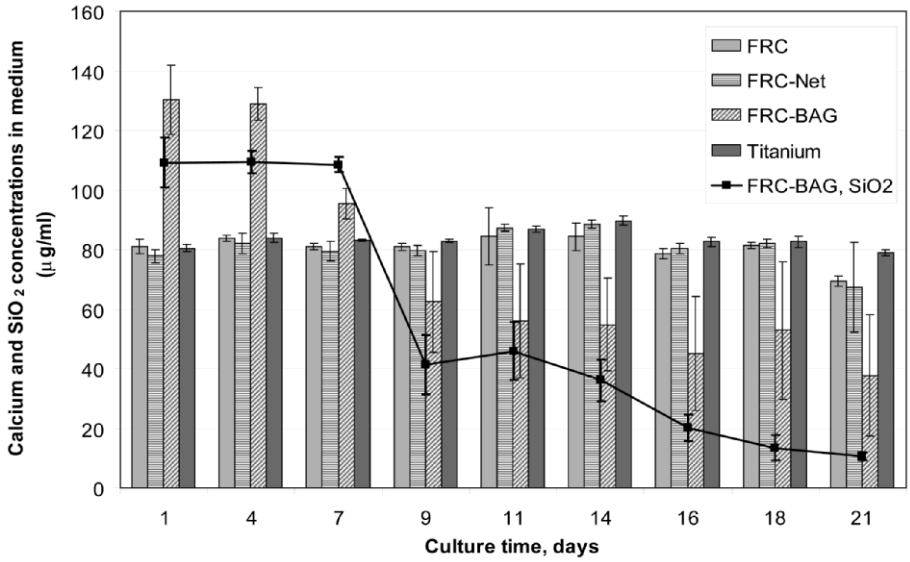

Figure 17. Evolution of calcium (columns) and silica (line) concentrations in culture medium. The calcium level in fresh culture medium is ~80 µg/ml. Error bars represent standard deviations.

6.3.2. Cell Proliferation

The proliferation of osteoblasts on different surfaces was measured over a period of 21 days. The cell activity on all the tested materials increased with time. Within the first week of culture there were no significant differences in proliferation, as indicated by the Alamar Blue assay (Figure 18). On day 14, however, the cell activity on FRC-BAG was significantly lower ($p < 0.05$) than on titanium and FRC. The cell activity on FRC-BAG also remained lower on day 21, albeit with no significant difference. The proliferation on the other three materials was equal throughout the experiment.

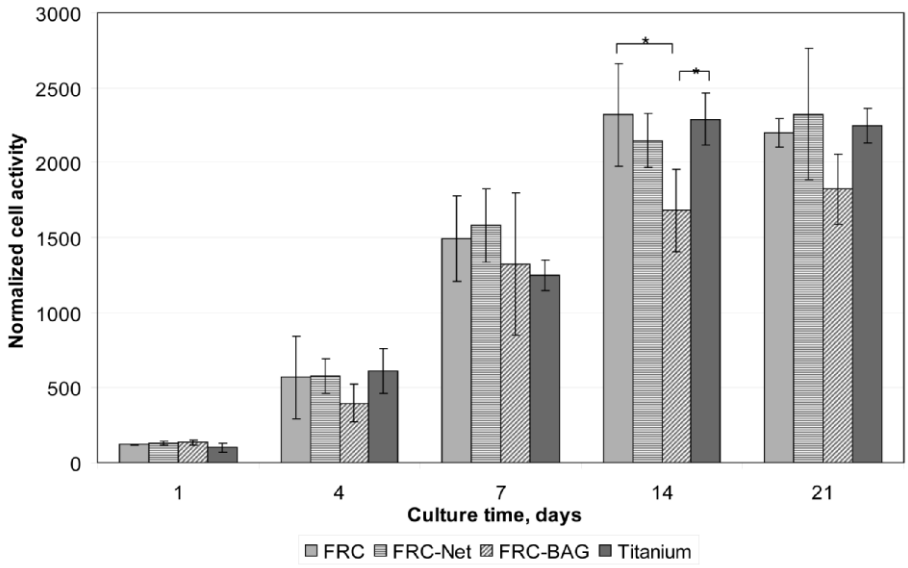

Figure 18. Cell proliferation with cultured substrates after 1, 4, 7, 14 and 21 days. Error bars represent standard deviations and * indicates a statistically significant difference ($p < 0.05$) between materials.

SEM micrographs (Figure 19) showed good cell proliferation and spreading over the material surfaces. A semi-confluent cell layer was formed by day 7, whereas a multilayer of cells with a collagen-rich matrix entirely covered all the substrate types by day 14. No differences among the materials were observed.

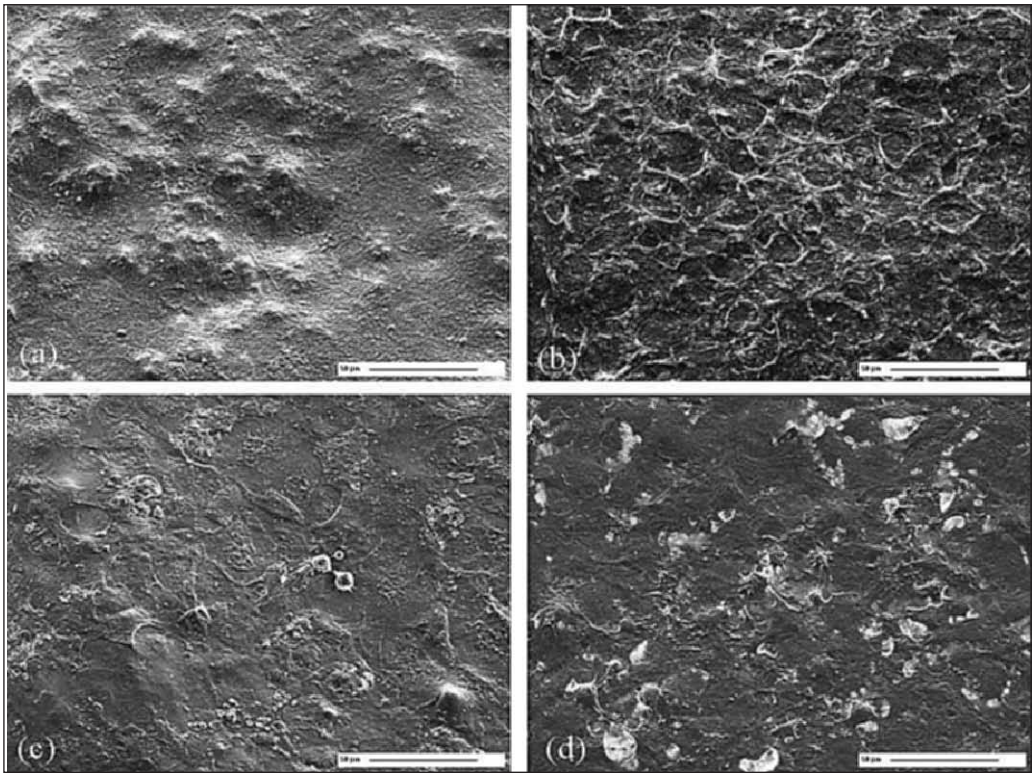

Figure 19. Scanning electron micrograph of osteoblast-like cells after 14 days of culture. (a) FRC, (b) FRC-BAG, (c) FRC-net, (d) Titanium.

6.3.3. Alkaline phosphatase activity

Alkaline phosphatase (ALP) activity was measured after 4, 7, 14, and 21 days of culture, and it increased with time (Figure 20). The maximal ALP activities on FRC, FRC-Net, and titanium were observed on day 21. FRC-BAG had already reached the maximal level on day 14, and on day 21 the activity was significantly lower than on the other materials ($p < 0.05$).

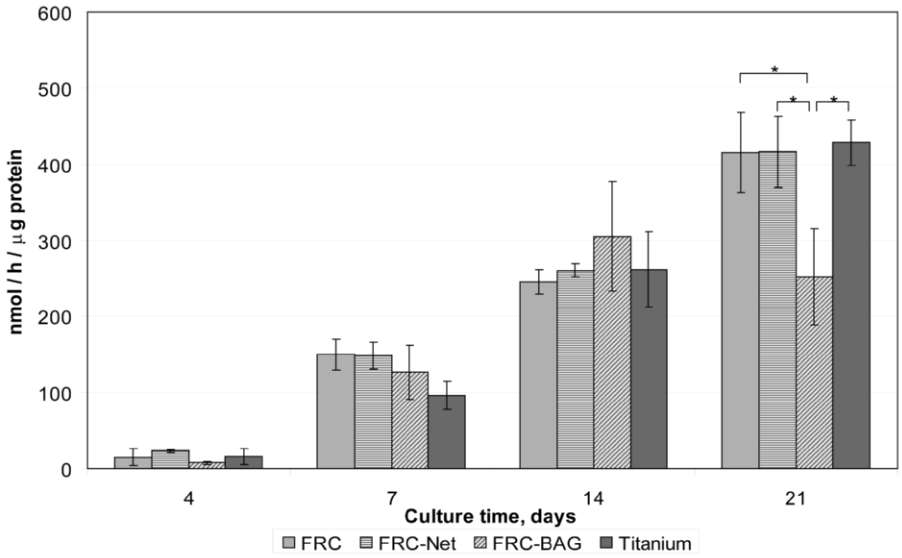

Figure 20. The evolution of ALP activities during three weeks' culture. Error bars represent standard deviations and * indicates a statistically significant difference ($p < 0.05$) between materials.

6.3.4. Gene expression

The progress of osteogenic differentiation is summarized in Figure 21. The gene expression profile of the cell stock used to seed the scaffolds showed clear signs of osteogenicity (ΔC_T, BSP = 1.85, ΔC_T, OC = -4.15).

Strong, and statistically significant ($p < 0.05$) induction of BSP was observed with all materials after 7 days in culture. In contrast, clear OC induction did not take place until day 14, although FRC and FRC-Net showed a slight induction already at 7 days. No further changes in the gene expression levels were observed, except with titanium, in which case the BSP and OC expression at 21 days was significantly higher than at 7 days and 14 days, respectively.

The fastest osteogenic differentiation seemed to take place on FRC. Specifically, statistically significant differences after 7 days were observed in OC expression when compared to titanium ($p = 0.008$), and in both the BSP and OC expression levels when compared to FRC-BAG ($p = 0.012$ and $p = 0.011$). In contrast, a prolonged differentiation process was observed on titanium, with a higher OC expression level than on any other tested material ($p < 0.015$) at 21 days. At that time, BSP expression on titanium also seemed to be increased compared to FRC-BAG ($p = 0.058$) and to FRC-Net ($p = 0.050$),

although with ambiguous statistics. No other differences among the tested materials were observed.

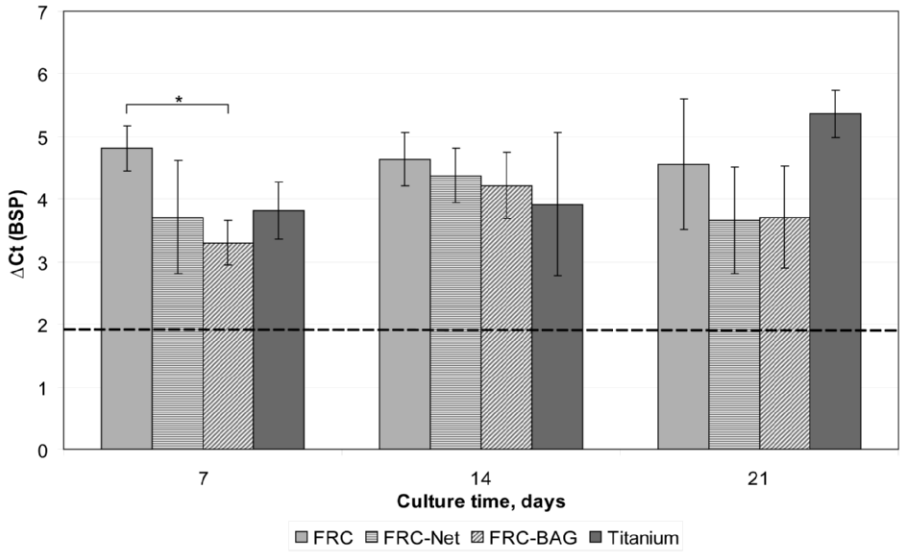

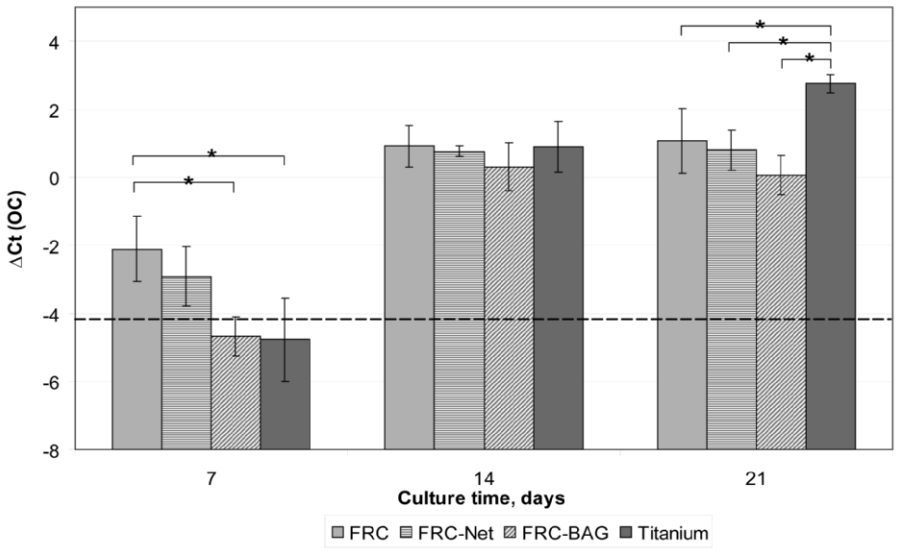

Figure 21. The progress of osteogenic differentiation, BSP (A), OC (B), during three weeks culture. The expression levels in the initial cell stock are marked with dashed lines. Error bars represent standard deviations and * indicates a statistically significant difference ($p < 0.05$) between materials.

6.4. Micro-CT analysis (IV)

Results of micro-CT analysis are shown in Figure 22. The new bone formation filled the space between the threads of both groups, while the bone volume showed a concurrent increase with the threaded bioactive FRC implants compared with the FRC implants without bioactive glass coating after 12 weeks (Figure 23).

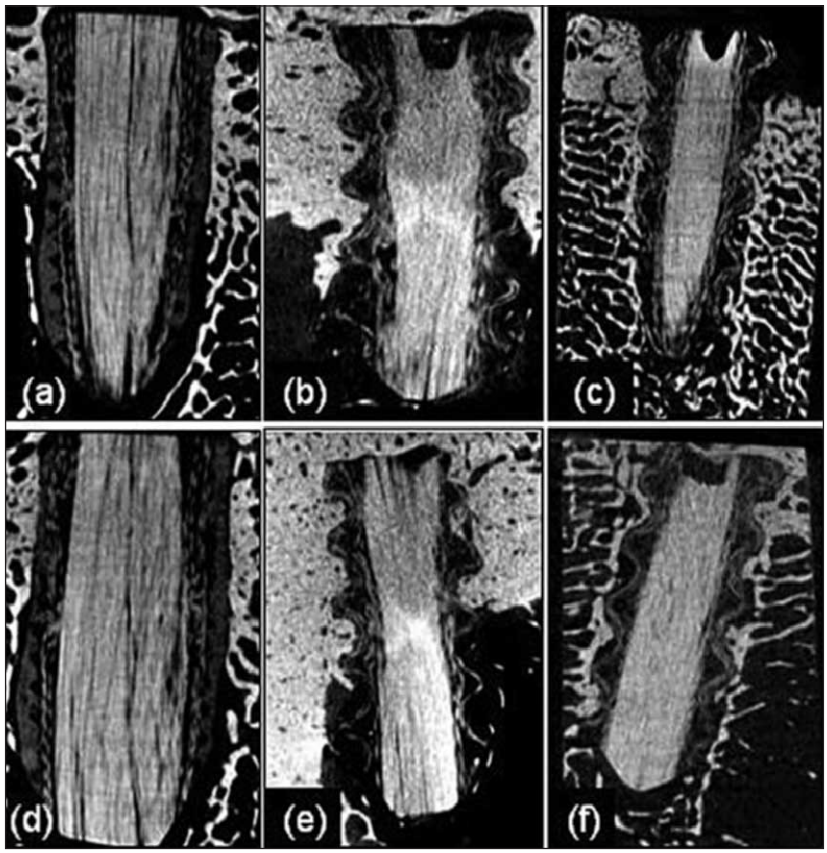

Figure 22. XCT images illustrate the bone growth in close contact with bioactive glass (BAG) coated non-threaded FRC implants (a and d), with sandblasted threaded FRC implants (b and e) and with BAG-coated threaded FRC implants (c and f) after 4 (upper row) and 12 weeks (lower row) of implantation.

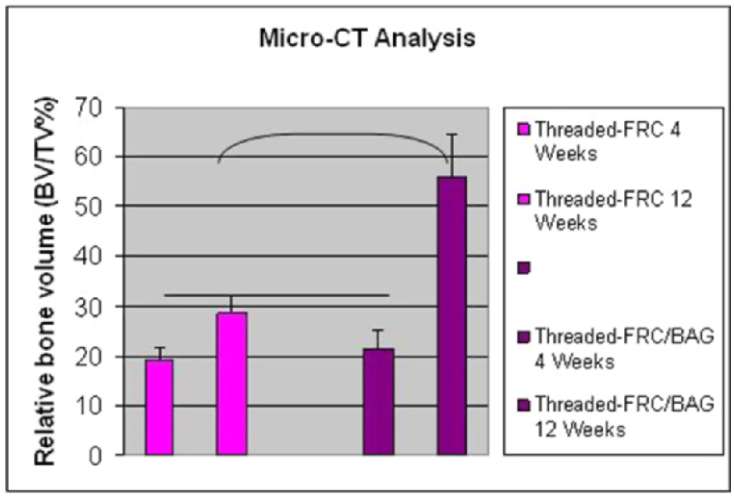

Figure 23. Mean values of relative bone volume between the threads of experimental threaded FRC implants.

6.5. Bone-bonding strength of FRC implant (IV)

Results of the push-out test are shown in Figure 24. Push-out strengths of threaded FRC/BAG implants after 4 and 12 weeks (463 and 676 N) were significantly higher than those of threaded FRC implants (416 and 549 N, $p<0.0001$), or non-threaded FRC-BAG implants (219 and 430 N, $p<0.0001$). No significant differences occurred between the threaded experimental implants after 4 weeks.

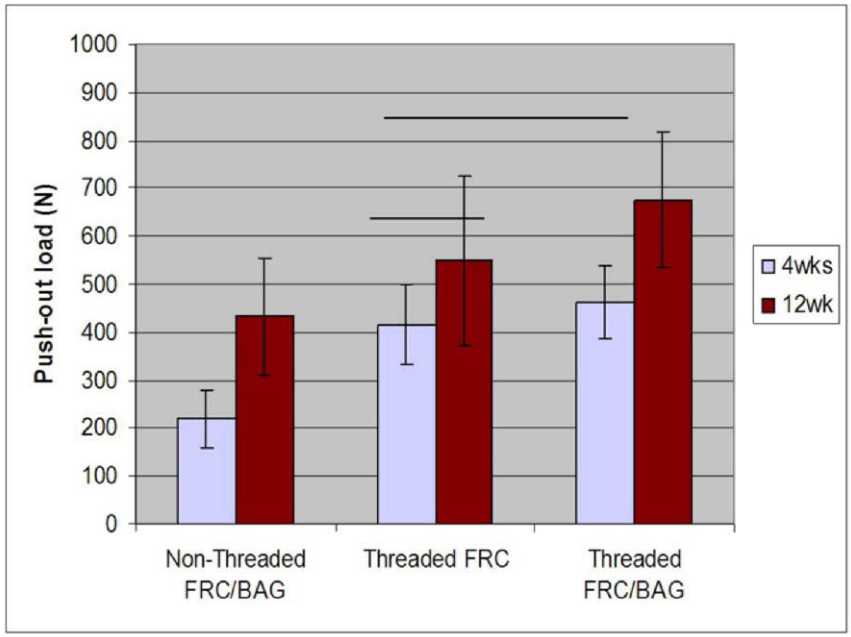

Figure 24. The mean push-out strength values of experimental FRC implants. Horizontal line above bars represents homogeneous subsets (Tukey post hoc test).

SEM analysis revealed that all FRC implants remained sound after the push-out test. In all threaded implants, fracture had occurred at the level of the thread crests. In the FRC/BAG implants, newly formed bone filled the thread areas, being in immediate contact with the bioactive coating (Figure 25), while in non-threaded FRC implants, fracture took place mainly at the implant-bone interface.

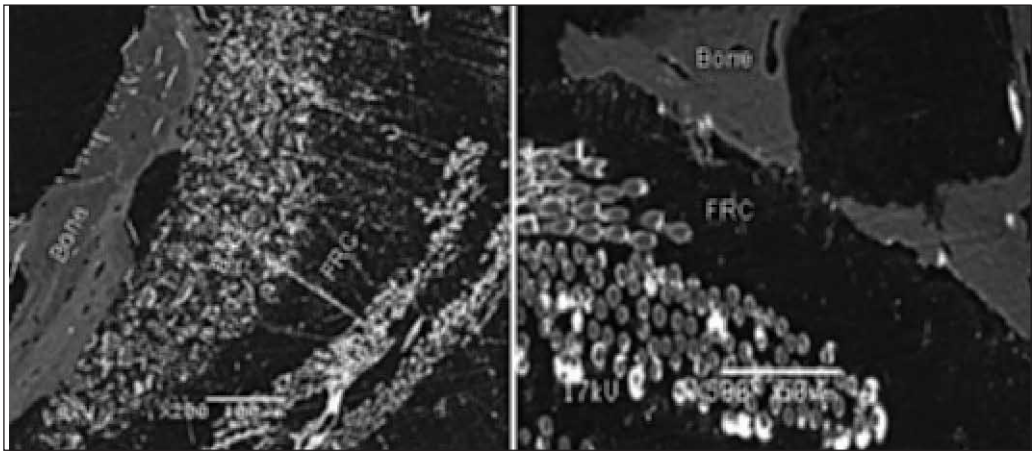

Figure 25. SEM micrographs of fracture surface of threaded FRC implants with and without BAG coating after push-out test. The fracture occurred within the bone and not at the bone-implant interface.

6.8. Histological and histomorphometry (V)

Table 7 illustrates the mean percentage of bone-implant contact (BIC) and standard deviations between experimental FRC implants and control implant at 4 weeks and 12 weeks. ANOVA revealed that BIC with different implants was statistically affected by time ($p<0.001$) and type of implant ($p=0.061$). BAG-coated FRC implant revealed the highest bone-implant contact at both time points even thought the difference was not statistically significant.

The healing period was uneventful for all experimental animals. No operative or postoperative complications were encountered.

Table 7. Bone-to-Implant Contact (BIC) of different implant types.

Healing Time	Implant Type	Minimum Value	Maximum Value	BIC (±SD)
4 wks	FRC	16.6	33.0	27.5 ± 5.1 [ab]
4 wks	Ti	12.7	31.4	19.3 ± 6.9 [a]
4 wks	FRC/BAG	19.2	55.1	33.1 ± 11.1 [abc]
12 wks	FRC	20.1	65.6	40.2 ± 15.3 [bc]
12 wks	Ti	21.0	65.4	41.8 ± 12.3 [bc]
12 wks	FRC/BAG	33.6	55.6	46.9 ± 9.0 [c]

[a] Same superscript for BIC values, letters indicates homogenous subset

Histological evaluation showed no signs of inflammation or bone resorption in surrounding host bone. Four weeks following the implantation (Figure 26), wound healing continued and new bone apposition was observed in all implants. The newly formed bone tissue extended from the cut bone surface into the chamber between the threads, but also woven bone appeared to be in direct contact with both blasted FRC and BAG-coated FRC surfaces (Figures 27 & 28).

After 12 weeks, the chambers between the implant threads is completely occupied with mature bone and haversian systems were readily identified in the compact bone in direct contact with both FRC surfaces.

BAG-coated FRC implant surface showed newly formed bone in direct contact with the implant surface, and uniformly distributed in the cortical portion and marrow spaces, while, only occasional contacts between bone trabecula in marrow spaces and blasted FRC and Ti implant surfaces were observed (Figures 26 & 28).

Newly formed bone was observed at the lateral border of the bony bed and it appeared to be continuous with the parent bone, indicating distance osteogenesis (Figure 29) (Davies, 1998). Woven bone was also present on the sand-blasted FRC and BAG-coated surfaces at a distance from the parent bone of the implant site, representing contact osteogenesis (Figure 29) (Davies, 1998). After 12 weeks, in both experimental and control implants, well matured bone had completely filled the gap between the implant threads and replaced most of the woven primary bone with lamellar bone.

EDX analyses support the mechanism of a gradual degradation of the bioactive glass coating and its integration with bone (Figure 8 in original publication).

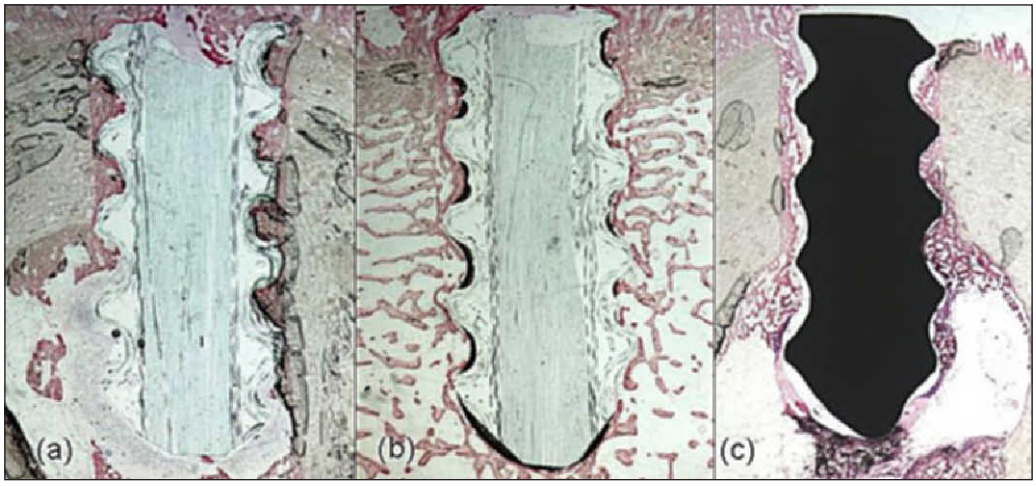

Figure 26. Histological pictures illustrating the bone growth between the threads of different implant types after 4 weeks of healing. (a) Threaded FRC, (b) threaded FRC/BAG and (c) threaded Ti.

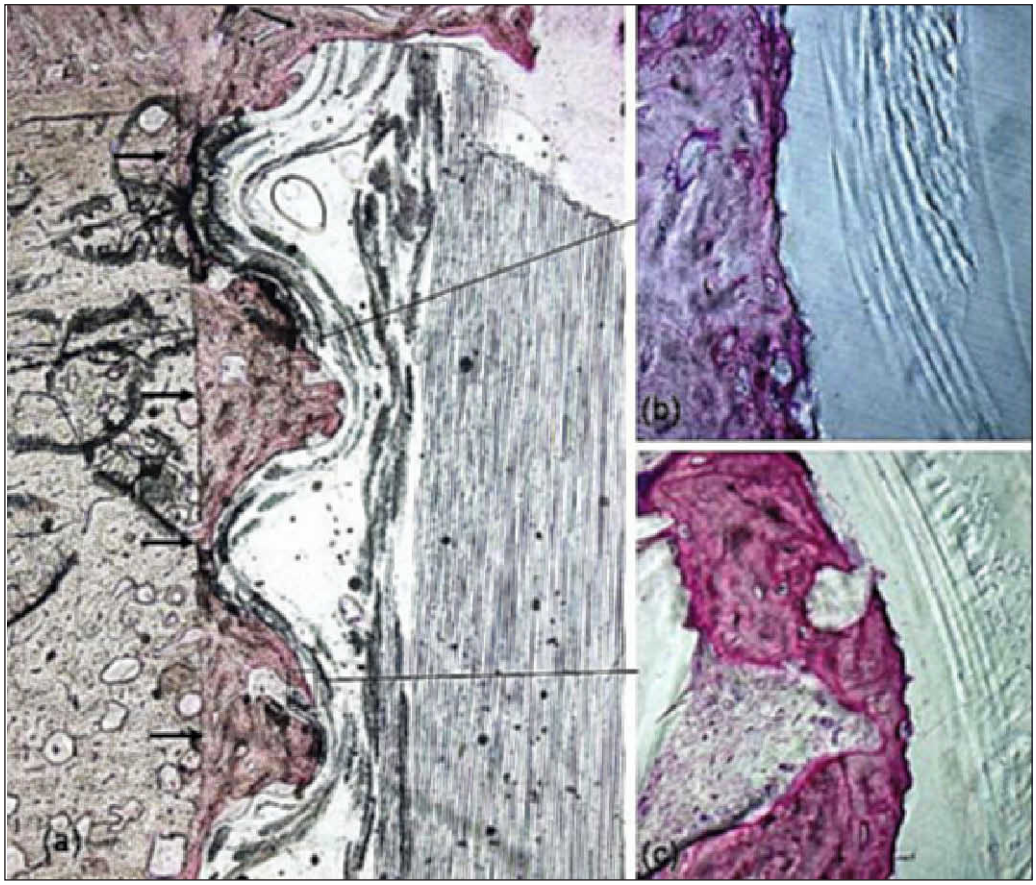

Figure 27. FRC device with surrounding tissue after 4 weeks of healing. Ground section. (a) Original mag. X 25. Large volumes of newly formed bone present at lateral border of the cut bony bed (arrows). (b and c) Woven bones penetrating the chamber to the blasted FRC surface. Original mag. X 400.

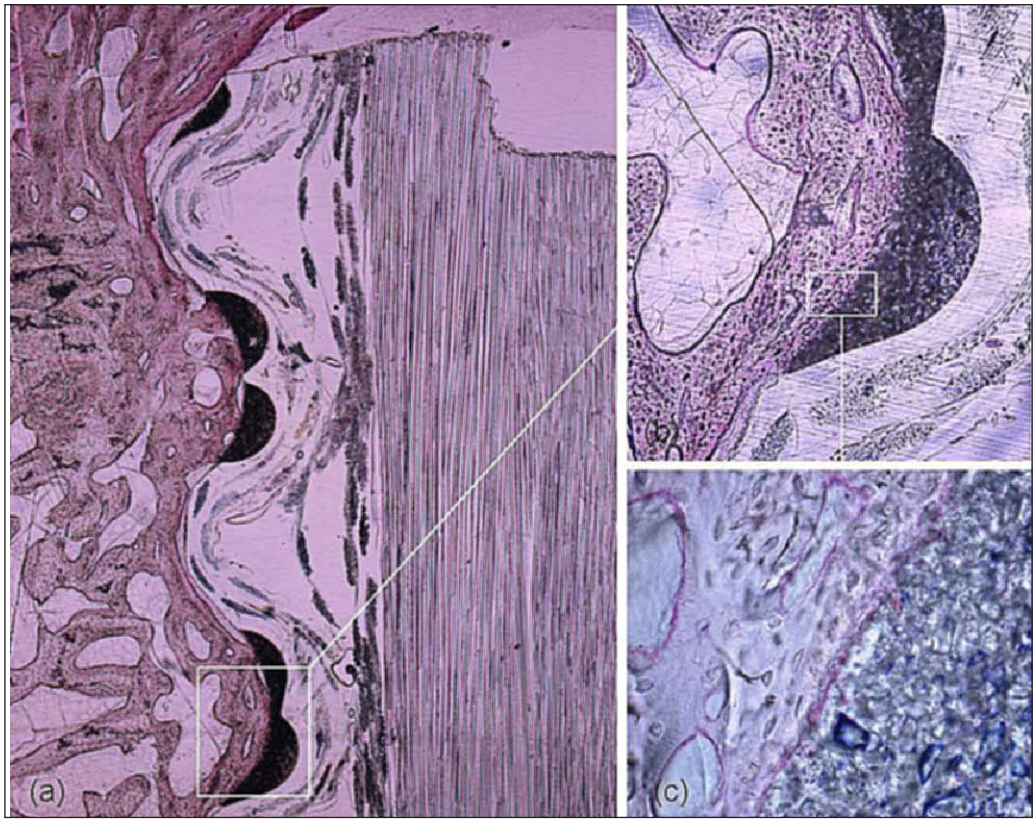

Figure 28. (a) Area between threads after 4 weeks of healing. Original mag. X 25. Newly formed bone penetrates to the area of the BAG-coated FRC surface. (b) Detail of Figure. 27a. The area between threads is comprised of a mix of woven bone and lamellar bone. Original mag. X 200. (c) Large mag. X 400.

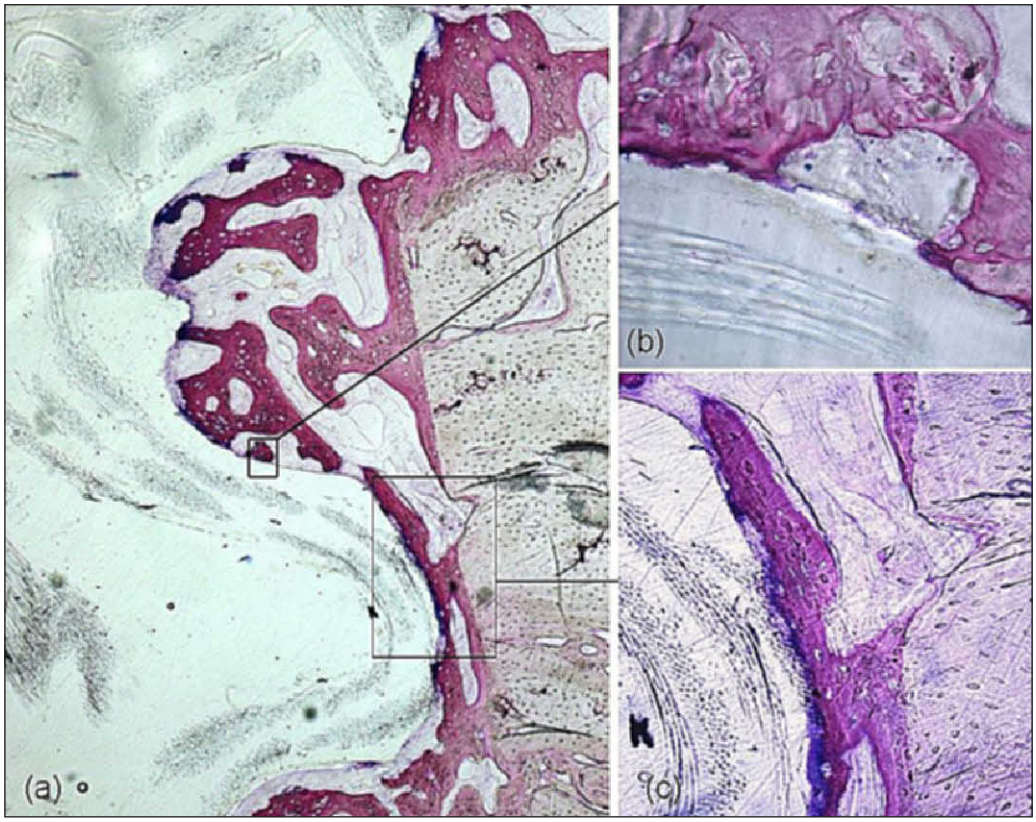

Figure 29. (a) The area between the threads represents 4 weeks of healing. Original mag. X 100. The newly formed bone present at lateral border of the bony bed appeared to be continuous with the parent bone (appositional bone formation). (b and c) Detail of Figure 28a. Original mag. X 200 and 400, respectively. Fig. 28 (b) Woven bone was also found on the blasted FRC surface (contact osteogenesis).

7. DISCUSSION

7.1. General discussion

Introduction of a new biomaterial for surgery requires a certain number of preclinical studies. This series of *in vitro* and *in vivo* studies aimed to evaluate the potential use of glass fiber-reinforced composites with photopolymerizable resin system as a dental implant. The main idea behind the hypothesis was that FRC has a lower modulus of elasticity, which is comparable to that of bone, and it may thus reduce undesirable high stress concentration on the cortical part and along the surface of the bone-anchored FRC implant. It may have better potential to distribute stresses to surrounding bone more favorably than the traditional titanium implants. Adding bioactive glass (BAG) particles to the FRC device was proposed to improve bone bonding and to enhance bone formation in the close vicinity of the implanted device.

Dental implants serve primarily as replacements for teeth, and designed to provide the strength appropriate for sustaining considerable loads. Therefore, when preliminarily evaluating the possible used of a novel FRC material as implant material, the bending and torsion properties and the degree of monomer conversion of FRC implant shaped test specimens were evaluated in study I.

In study II, load-bearing capacity of threaded FRC devices using the push-out test in a simulated bone structure was evaluated and compared to conventional titanium with an experimental thread design and commercially available titanium dental implants. The purpose was also to evaluate the possibility of using bioactive glass (BAG) granules on the experimental FRC devices in terms of their mechanical behavior.

Although the mechanical properties of FRC anchoring devices have been found to be comparable to those of titanium implants, further studies are needed to explore the biological behavior of bone- FRC implant devices. Consequently, in study III, the proliferation and osteogenic potential of bone-marrow derived osteoblast-like cells on FRC substrates were evaluated.

The surface of an implant determines its ultimate ability to integrate into the surrounding tissue. Therefore, the study is based on a working hypothesis that a blasted FRC surface and/ or the addition of BAG particles to the FRC surface promotes osteoblast behavior on FRC. However, the results achieved in static cell culture conditions cannot directly be extrapolated to clinical conditions. Studies IV and V were conducted [in order] to obtain more information about bone-bonding forces of FRC implants, and to evaluate the bone tissue responses of the FRC implant in vivo.

7.2. Mechanical test

7.2.1. Bending and torsional tests

In a clinical environment, dental implants are subjected to multidirectional forces (Rangert *et al.* 1995; Mao *et al.* 1996; Richter 1998). Forces can have either vertical or horizontal components, but also inclined and torsional forces may exist (Rangert *et al.* 1995).

Cantilever bending refers to a loading arrangement in which one of the specimens is rigidly fixed while the other end is completely free. The bending moment due to forces deviating from the direction of the implant axis can produce higher stress in the implant and implant-bone interface than the direct axial load (Rangert *et al.* 1995; Morgan and James 1995). The excessive bending moments may cause stress concentration and micro-fractures in alveolar bone, and even implant fractures. Therefore, in addition to the fact that the modulus of elasticity of the implant material should be closer to the bone, the implant material must also exhibit mechanical properties which will ensure a long-lasting function. In the study (I), the test set-up was designed to simulate simple clinical loading conditions for the dental implant.

The currently tested resin materials may also be acceptable for use in dental implants, especially if they have been polymerized to high DC%. It is well known that a higher DC% results in better mechanical properties for the polymer and composite material than a lower DC% (Lassila *et al.* 2004).

The higher DC% can be obtained by lengthening the polymerization time and increasing the polymerization temperature. Improvement in mechanical properties by the increased DC% are related to the increased cross-linking density, which increases the number of covalent bonds between polymer backbones and lowers the amount of residual monomers that could plasticize the polymer matrix (Evans *et al.* 2002; Palussiere *et al.* 2005; Andreassen *et al.* 2004). The present study also confirmed this by showing substantial improvement in the bending and torsional properties of the specimens with high DC%. A three times higher load to failure for implant specimens was observed in group D compared to group A. The quantity of leachable residual monomers decreases with the increasing DC%. Thus, besides the improved strength, the high DC% obviously improves the biocompatibility which is required for the implant materials.

In groups A-D, failure occurred in the form of cracks and delamination of resin-preimpregnated prepregs (interfacial failure), followed by growing cracks at the interface between prepregs (Figure 5 in original publication). This problem could be overcome by improving the interfacial adhesion of the prepregs used in specimen fabrication, or alternatively, by using a different fabrication process as was used in groups E and F.

Specimens in groups E and F were prepared to avoid delamination by changing the fabrication process. In group E, the specimens were coated with fiber weave to encapsulate the unidirectional fibers together (Figure 6 in original publication), whereas in group F, the specimens were made of manually impregnated fibers as one roving of large size. The four times higher load to failure obtained in group E compared to Group A suggests that the fiber weave effectively protected the unidirectional fibers against delamination.

This *in vitro* study showed that the mean static load to failure of specimens in all groups was above the previously reported maximum incisal biting force, whereas the mean load of failure for groups D, E and F were beyond the reported maximum posterior bite force (Van Eijden 1991). However, flexural fatigue studies are needed to simulate the dynamic loading conditions of the masticatory system.

Torsional loading produced maximum shear stress and twisted the structure along the neutral axis. Shear stress increases as a function of distance from the neural axis. In torque, the specimens in groups A, B, C and D exhibited twisting in the very first moment of loading, and delamination occurred before torque was registered. Therefore, no torque data were available for the specimens of groups A-D. Encapsulation of unidirectional FRC with a fiber weave (Group E) improved resistance to torque. Since this specimen design showed the best mechanical properties in our study it seems to have the greatest potential also for *in vivo* studies.

7.2.2. Load-bearing capacity of threaded FRC (II)

The screw thread of a dental implant plays an important role in the initial stability of the implant and reduces micro-motion to optimize the healing period before a safe functional loading can be exerted.

Study II was conducted to determine the load-bearing capacity of bone-anchored FRC devices by using the push-out test before their evaluation in a living bone environment.

Various techniques have been used to examine the mechanical strength of medical devices. The choice of these tests depends on the clinically most significant failure mode of implants. The strength of a FRC composite device is limited by the strength of its weakest component. However, the load-bearing capacity of threads in screw-shaped FRC devices under vertical load has not been known. In this study, we chose to embed the experimental devices into dental plaster instead of bone. A similar method has been used by Mattila *et al.* (2006) to evaluate the effect of surface texture as a retention property of the implant. With this method, it is possible to test the load-bearing capacity of devices in an equivalent environment, without having the problem of standardizing the porous bone structure.

The result of the push-out tests conducted on FRC specimens with FRC threads revealed a load approaching 1300 N. These values were almost double those achieved with identical threaded titanium (IV, control) devices. Fracture always occurred in the plaster; no thread failures were observed. The reason for the higher push-out force of FRC specimens is obviously related to the lower modulus of elasticity of FRC (40 GPa) compared to titanium (120 GPa) (Yuehuei 2000). In the vertical force of the load-bearing test, the FRC reduced the compressive radial stress at the plaster-device interface and around the threads of the FRC specimens. The stress was distributed more evenly throughout the FRC structure and to the surrounding area compared to the titanium device.

The threaded FRC devices aim to achieve fixation through mechanical interlocking with the surrounding bone, while the bioactive coatings are used to achieve a biological bond with bone. However, a certain degree of surface roughness is required to obtain mechanical interlocking ever for the coated devices. The cylindrical non-threaded FRC devices with BAG coating (Group I) had the most irregular surface with noticeable pits and fissures, while the threaded FRC specimens with BAG coating (Group III) showed a rough surface with very small pits. The threaded FRC devices (Group II) without any surface modification and the control titanium specimens had smooth surfaces. The Straumann dental implants, which were also used as a reference, had a modified surface (SLActive surface). The SLA surface has been demonstrated to have better bone-bonding properties than the previously used titanium plasma-sprayed (TPS) surfaces (Buser *et al.* 1999). In terms of the push-out force, the threaded FRC devices used in this study performed as well as the Straumann SLA implants.

The study also showed that in all threaded FRC devices, the measured push-out forces exceeded the reported maximum bite force (van Eijden 1991), but were lower than the strength of the weakest part of the threaded FRC devices. Some failures occurred in the threads when the push-out force was higher than 2,500 N. Such high forces were registered only with FRC devices additionally coated with BAG, and when extra retention was provided by supplementary retention grooves (Group III). In the non-threaded specimens, failure occurred due to detachment of the BAG granules from the surface of the FRC device. Hence, the interface between the BAG granules and the FRC structure was the weakest link in the non-threaded specimens.

Thus, although the bond between the FRC device and bone may be improved through the use of a bioactive material on the device surface, a significant limitation remains in the interfacial bond between the bioactive particles and the FRC device. In the non-threaded devices, the FRC/BAG interface was assumed to be able to resist compressive stress but not shear stress. However, in the threaded FRC specimens with BAG coating, the BAG granules were partly in compression with respect to the FRC surface, which provided a better environment for the BAG granules. It may be assumed that the interface between

bone and FRC device can tolerate higher loads than those described in this study since the bioactive glass particles will form an apatite surface layer on the implant-to-bone interface, which can lead to biological bone bonding (Moritz *et al.* 2004).

7.3. Cell response

Adhesion of cells to a biomaterial surface can be a major factor mediating its biocompatibility. This cell adhesion to the surface allows strong attachment of the surrounding tissue to the biomaterial.

In study III, we have shown that osteoblast attachment, proliferation and differentiation on the BisGMA-TEGMA polymer with E-glass fiber reinforcement is comparable to that observed on titanium. An additional aim of the present study was to analyze the osteoblast response to FRC, with or without BAG coating. Furthermore, the effect of exposed E-glass fibers was evaluated.

The introduction of a new biomaterial for surgery requires a certain number of preclinical studies. Since an implant must be firmly lodged in bone tissue, it is desirable that an evaluation of its biocompatibility be made using cells cultured from bone tissue.

The three different FRC substructures used in this study were made of pBis-GMA-pTEGDMA copolymer, which is already used clinically as approved bone cement (Andreassen *et al.* 2004; Evans *et al.* 2002; Palussière *et al.* 2005). All the tested specimens were blasted with similar sized aluminum oxide particles to produce comparable surface roughness on each material. A surface can be considered rough when it has peak heights greater than 2 μm but less than 10 μm (approximately equal to the cell length), and this has been shown to increase osteoblast activity (Ong *et al.* 1998). The blasting process also exposed some of the E-glass fibers on the FRC-Net, but this did not show any adverse effects on the cultured cells. Aluminum oxide particles were used for the blasting as it has been shown that the presence of alumina particles on blasted titanium does not interfere with bone apposition in *in vivo* conditions (Wennerberg *et al.* 1996). The higher final surface roughness of FRC specimens compared to titanium is due to the softness of the polymer surface, resulting in higher abrasion of the surface.

SEM observation showed that the cultured cells proliferated on all the blasted surfaces, and eventually formed multicellular layers entirely covering the specimens. Within 21 days of culture, no visible differences could be noted among different FRC substrates and titanium, indicating that the tested FRCs are cytocompatible materials with a cellular response similar to that of titanium.

Alkaline phosphatase activity, bone sialoprotein, osteocalcin production and mineralizing phenotype are important parameters typically used as markers of osteoblastic

differentiation. The normal differentiation process includes a reciprocal relationship between proliferation and differentiation of osteogenic cells (Malaval *et al.* 1994; Stein *et al.* 1990). Accordingly, the cells on FRC-BAG stopped expanding and their ALP activity reached peak value during the second week of culture. Furthermore, their gene expression profiles increased to levels similar to those on the other surfaces, and the cells started to mineralize more rapidly than the cells seeded on the other materials. The enhanced differentiation cascade with FRC-BAG is probably related to Ca, PO4, and Si ions initially released from the BAG (Hench *et al.* 2004; Radin *et al.* 2005). The osteoblasts cultured on FRC-BAG showed a different trend in the calcium and silicon content of the culture medium compared with the other materials. The Ca and Si ions released from the bioactive glasses are known to stimulate the osteoblastic function and maturation (Yao *et al.* 2005). Hench and West (1996) have proposed that the release of soluble silica from the surface of bioactive glasses might be at least partially responsible for stimulating the proliferation of bone-forming cells on bioactive glass surfaces. However, the accumulating mineral phase inhibited further BAG dissolution, resulting in rapidly decreasing silica concentrations.

The results of this study support the initial working hypothesis that the addition of BAG particles promotes osteoblast behavior on FRC. However, the results achieved in static cell culture conditions cannot be directly extrapolated to clinical conditions.

7.4. Bone-bonding strength of FRC implant

The mechanical properties of FRC equal or exceed those of the materials which are, or have been, used in dental implants, while the elastic modulus of FRC resembles the modulus of bone. Despite their encouraging mechanical behavior, the bone-bonding properties of FRC implants are not known.

Study IV describes the biomechanical characteristics of bone bonding with FRC implants. Bone trabeculae were clearly visible in the micro-CT scans around all the experimental FRC implants. The fact that new bone apposition was detected between the implant threads suggests good biocompatibility of the FRC implants. The enhanced bone anchorage of BAG-coated FRC implants was not surprising as the BAG used in this study has been shown to promote bone formation in many previous investigations (Aitasalo *et al.* 2001; Cordioli *et al.* 2001; Norton and Wilson 2002). However, with the exception of measuring direct bone-to-implant contact, investigation of the trabecular bone structure around implants with micro-CT alone is not a very reliable method for the characterization of bone structure.

Brånemark noted that pull-out and push-out tests measure peri-implant bone quality, since, by definition, the bone surrounding the implant fractures during the experiment

(Branemark *et al.* 1998). Although the push-out test measures the mechanical properties of bone around the implant and the strength of the coating-implant interface rather than measuring the shear strength of the bone-implant interface, from a clinical perspective, push-out data still provide valid information about how strongly an implant is anchored in the bone.

The present study shows a statistically significant improvement in the interfacial bond strength of the FRC/BAG implant with increasing healing time. It is unlikely that the difference in bone bonding is related to differences in surfaces topographies and surface volume as the non-coated FRC implants were moderately roughened with sand blasting. The better bonding strength of the BAG-coated FRC implant is rather related to the surface activity of BAG and ionic exchange at the implant bone interface. The presence of BAG is known to be conductive to bone formation and also to improve bone quality in the close vicinity of the coated implant (Moritz *et al.* 2004). The differences in bonding strength between non-threaded and threaded FRC implants are related to implant design (Bolind et al. 2005). Furthermore, the total bioactive surface area was larger in threaded FRC implants due to the larger implant surface, which could have further improved bone quality at the implant bone interface.

The push-out failure site was primarily in the bone tissue, not in the interfacial region, indicating that the interfacial strength was stronger than the newly formed bone tissue itself. This provided further evidence of good fixation between FRC surface and bone tissue. However, in non-threaded BAG-coated implants, failure occurred at the coating-bone interface, which can be related to poor initial stability, and the fact that, in the FRC implant, the interface is assumed to be able to resist compressive stress but not high shear stress. However, in the threaded FRC specimens with or without BAG coating, the interface was partly compressed with respect to the FRC surface, thus providing a better environment for the bone-implant interface. It should be noted that all the experimental implants were inserted with the press fit protocol. Thus, the implants had poor primary stability, and their push-out strength was derived from bone apposition at the bone-implant interface.

There was no evidence of breakdown or change in thickness of the BAG coating. The good mechanical and biological responses suggest that the BAG embedded in the composite resin, enhances the biological performance of FRC implants.

Interestingly, uncoated and sandblasted FRC implants also showed good osseointegration. This finding corresponds to the results obtained in an *in vitro* cell culture study, which revealed good osteoblast proliferation and bone formation on the uncoated and BAG-coated FRC specimens.

7.5. Bone response

A safe and predictable tissue response is a fundamental requirement for all biomaterials in medical use. For these reasons, the introduction of a new biomaterial for clinical application requires a certain number of preclinical studies. Good bone bonding (osseointegration) is essential for implant materials in the bone environment. The osseointegration of an implant biomaterial depends on its ability to conduct bone growth. For example, bone conduction is not possible on certain materials such as copper and silver (Albrektsson 1995). However, bone conduction can be seen with materials whose biocompatibility is not regarded as optimal for an implant material, e.g. stainless steel (Johansson et al. 1992), and with materials with high biocompatibility such as commercially pure titanium and its alloys (Steinemann 1998). The present study was established to explore bone response to FRC implants. A further aim was to study the possibility of enhancing the osteoconductivity of FRC implants by adding BAG granules to the subsurface area of the implants.

The release of residual monomers from BisGMA-TEGMA polymer may influence the biocompatibility of polymer implants (MacDougall et al. 1998). Residual monomer can also cause allergic reactions if there is sensitization for the monomers, as has been noticed in clinical dental practice (Pfeiffer & Rosenbauer 2005). Because of this, the FRC implants should have an optimum degree of monomer conversion. This can be obtained by lengthening the photopolymerization time in combination with heat-induced post-curing (Ferracane & Condon 1992) before implantation.

A degree of monomer conversion of approximately 90% of the polymer could be achieved by photopolymerization in a vacuum and post-curing for 24 hours at 120° C (Study I). This temperature is close to the glass transition temperature (T_g) of pBisGMA-pTEGDMA-copolymer. With further storage in water the residual monomers are leached out from the FRC implants, thus improving the biocompatibility of the polymer matrix.

A previous experimental study aimed to evaluate the tissue/implant interface of epoxy-resin replicas of cylindrical titanium implants. The replicas were coated with a 90-120nm thick layer of pure titanium and implanted into the edentulous premolar region of dog mandibles (Listgarten et al. 1992). Histological evaluation clearly showed that bone grew in direct contact with the coated replica. This study clearly demonstrated that bulk material characteristics are mainly responsible for mechanical and structural properties, while the surface characteristics are responsible for biocompatibility through interfacing with the biological environment.

Our study showed that the polymer surface can guarantee equal bone formation after 4 and 12 weeks of healing with titanium. Neither sand-blasted FRC implants nor BAG-coated FRC implants showed toxicity to the pig bone tissue during the 12-week healing period. The direct attachment of osseous tissue to the BisGMA-TEGMA polymer with

E-glass fiber reinforcement indicates that the FRC implant is biocompatible in the bone environment.

The significantly greater percentage of BIC adjacent to BAG-containing FRC than in the roughened FRC or titanium implants is clearly related to the reactivity of BAG.

Our findings about BIC in titanium implants are in agreement with those obtained previously with large-grit sand-blasted titanium implants, showing 30% to 40% mean bone contact at 3 and 6 weeks of implantation in the tibia of miniature pigs (Buser et al. 1991).

Bone healing around the implants is site-related, as bone quantity and quality can differ greatly even within the same bone. The osseointegration of oral implants can also be affected by the presence of gaps between implant and bone, and by pre-existing bone that is damaged by surgical procedures (Brunski 1999).

This histological and histomorphometric study supports our previous findings of increased bone bonding with BAG-containing FRC implants. The results showed that biochemical bonding with the FRC/BAG implant surface occurs already 4 weeks after implant insertion. Thus, the addition of BAG significantly improves the performance of FRC implants: the bone bonding surface area is larger and bonding strength higher than with sand-blasted FRC or control titanium implants. Delamination of BAG does not challenge osseointegration as BAG particles are embedded beneath the polymer surface. The mechanical bone bonding study showed that push-out failure takes place within the bone tissue but not in the bone-to-implant interface.

The presence of Ca and P on the outer surface of the FRC/BAG implant supports the observed mechanism of a gradual dissolving of the bioactive glass particles and CaP precipitation on the polymer surface (Jakkola et al. 2004). The fact that the BAG will eventually resorb completely is non-essential, as when the implant is integrated into bone, long-term fixation will be achieved through bone ingrowth into the porous surface structure of the FRC implant.

7.6. Future perspectives

In the future, flexural fatigue studies of the implant-bone system are needed to simulate the dynamic loading conditions of the masticatory system. Further studies are needed to evaluate the bone remodeling process and the mechanical strength of the FRC implant under loading condition.

In dentistry, the implanted device interfaces with a variety of tissues (epithelial, connective tissues, and bone). By understanding the FRC implant surface characteristics which are optimal for each of these tissues, investigators will be able to design better implants by customizing specific regions of the implant for each tissue type.

8. CONCLUSIONS

1. The failure forces of the experimental FRC specimens with an average dental implant diameter exceeded the reported maximum static human bite forces. In addition, encapsulation of continuous unidirectional glass fibers with a fiber weave, improves FRC specimens' resistance against torsional and bending forces.

2. The threads of FRC bone-anchoring devices can withstand static load values comparable to human maximal bite forces without fracture.

3. The experimental FRCs showed no signs of cytotoxicity, and the osteoblast proliferation and enhanced mineralization on their surface were similar to those on commercially pure titanium. Furthermore FRC with BAG coating showed enhanced osteogenic differentiation.

4. All experimental FRC implants showed improvement in push-out strength with increasing healing time, while the addition of BAG improves the push-out strength of FRC implants after 12 weeks' implantation.

5. FRC implants have a bone response comparable to titanium implants. The addition of bioactive glass granules improves the bone response to FRC implants.

With critical attention to technical design and surgical technique, FRC material can be successfully applied for dental implants.

ACKNOWLEDGEMENTS

This research was carried out at department of Prosthetic Dentistry and Biomaterials Science, Institute of Dentistry, University of Turku, Finland between March 2005 and August 2008.

It has been said that the doctoral dissertation process is about identifying paths and breaking barriers. For my part, this process has been challenging, but still enjoyable, I would like to thank the following people who made this work possible and supported me in both identifying the paths and breaking the barriers.

My supervisors, Prof. Timo Närhi, for his guidance and encouragement over the past four year, Prof. Närhi, who also supervised me during the ITI clinical fellowship. Additionally, I am very grateful to my second supervisor and head of Department of Prosthetic Dentistry & Biomaterials Science, Prof. Pekka Vallittu, for giving me the opportunity to do my doctoral thesis on this interesting topic, as well as for the ideas and supportive discussions.

I would like to thank Lippo Lassila for his help, especially with statistic analysis. I also want to acknowledge my co-authors in the cell culture laboratory, especially Anne Kokkari. I also owe thanks to my co-authors, Niko Moritz and Teemu Tirri. And not to forget my other colleagues for contributing to creating a friendly and pleasant atmosphere-thanks for everything.

I would like to thank also Dr. Sadullah Uctasli for his kind help in the arrangement of the animal experiment in Turkey, and Dr. Eralp Akca for his help and assistance during the surgical part of the study.

Thanks to the official pre-examiners of the thesis, Docent Pekka Laine from Helsinki University Central Hospital and Prof. Albert Feilzer from Academic Center for Dentistry Amsterdam (ACTA) at University of Amsterdam.

I would also like to thank Professor Flemming Isidor from School of Dentistry at University of Aarhus for accepting the invitation to function as my opponent at the public examination.

My appreciation goes to International Team for Implantology (ITI) foundation for the research scholarship, and for granting me the dental implant courses and seminars. This work has been carried out within the Bio- and Nanopolymers Research Group of the Academy of Finland and was partially funded by the Finnish National Technology Agency (TEKES).

Finally, I thank my Libyan friends in Finland for their support at the first stage of my PhD study. And above all, my thanks go to my parents, my wife and my kids for all their unremitting love and support.

Turku, June 2008

REFERENCES

Adell R, Lekholm U, Rockler B, Brånemark PI. (1981) A 15-year study of osseointegrated implants in treatment of the edentulous jaw. Int J Oral Surg. 10:387-416.

Aitasalo K, Kinnunen I, Palmgren J, Varpula M. (2001) Repair of orbital floor fractures with bioactive glass implants. J Oral Maxillofac Surg. 59: 1390-95.

Albrektsson T, Hansson HA, Ivarsson B. (1985) Interface analysis of titanium and zirconium bone implants. Biomaterials. 6: 97–101.

Aldini NN, Fini M, Giavaresi G, Torricelli P, Martini L, Giardino R, Ravaglioli A, Krajewski A, Mazzocchi M, Dubini B, Ponzi-Bossi MG, Rustichelli F, Stanic V. (2002) Improvement in zirconia osseointegration by means of a biological glass coating: An *in vitro* and *in vivo* investigation. J Biomed Mater Res. 61:282-9.

Alexander H. (1996) Composites. In: *Biomaterials science*. BD Ratner, AS Hoffman, FJ Schoen, JE Lemons, editors. Academic Press, San Diego.

Andreassen GS, Hoiness PR, Skraamm I, Granlund O, Engebretsen L. (2004) Use of a synthetic bone void filler to augment screws in osteopenic ankle fracture fixation. Arch Orthop Trauma Surg. 124: 161-5.

Asmussen E, Peutzfeldt A. (1990) Mechanical properties of heat treated composite resin inlay/onlay technique. Scand J Dent Res. 98:564-7.

Balkenhol M, Wöstmann B, Rein C, Ferger P. (2007) Survival time of cast post and cores: a 10-year retrospective study. J Dent. 35:50-8.

Baron M, Haas R, Baron W, Mailath-Pokorny G. (2005) Peri-implant bone loss as a function of tooth-implant distance. Int J Prosthodont. 18:427-33.

Behr M, Rosentritt M, Lang R, Handel G. (2001) Glass fiber-reinforced abutments for dental implants. Clin Oral Implants Res. 12: 174-8.

Berglundh T, Persson L, Klinge B. (2002) A systematic review of the incidence of biological and technical complications in implant dentistry reported in prospective longitudinal studies of at least 5 years. J Clin Periodontol. 29:197-212.

Bevelander G. (1971) Connective and supporting tissue. In: Outline of histology. Mosby, Houston. 37-49.

Bolind PK, Johansson CB, Becker W, Langer L, Sevetz EB, Albrektsson TO. (2005) A descriptive study on retrieved non-threaded and threaded implant designs. Clin Oral Implants Res. 16:447-55.

Bonucci E. (2000) Basic composition and structure of bone. In: Mechanical testing of bone and the bone-implant interface. An YH and Draughn RA., editors. CRC Press, Boca Raton. 3-21.

Bouillaguet S, Schutt A, Alander P, Schwaller P, Buerki G, Michler J, Cattani-Lorente M, Vallittu PK, Krejci I. (2006) Hydrothermal and mechanical stresses degrade fiber-matrix interfacial bond strength in dental fiber-reinforced composites. J Biomed Mater Res B Appl Biomater. 76:98-105.

Braga RR, Cesar PF, Gonzaga CC. (2002) Mechanical properties of resin cements with different activation modes. J Oral Rehabil. 29: 257-62.

Brånemark PI, Hansson BO, Adell R, Breine U, Lindström J, Hallén O, Ohman A. (1977) Osseointegrated implants in the treatment of the edentulous jaw. Experience from a 10 year period. Scand J Plast Reconstr Surg Suppl. 16: 130-6.

Brånemark PI, Zarb GA, Albrektsson T. (1985) Tissue-integrated Prostheses: Osseointegration in Clinical Dentistry. Chicago: Quintessence.

Branemark R, O¨ hrnell LO, Skalak R, Carlsson L, Branemark PI. (1998) Biomechanical characterization of osseointegration: an experimental *in vivo* investigation in the beagle dog. J Orthop Res. 16:61-9.

Buser D, Nydegger T, Oxland T, Cochran DL, Schenk RK, Hirt HP, Snetivy D, Nolte LP. (1999) Interface shear strength of titanium implants with a sandblasted and acid-etched surface: a biomechanical study in the maxilla of miniature pigs. J Biomed Mater Res. 45:75-83.

Chang YS, Oka M, Nakamura T, Gu HO. (1996) Bone remodeling around implanted ceramics. J Biomed Mater Res. 30:117-24.

Chang YL, Stanford CM, Wefel JS, Keller Jc. (1999) Osteoblastic cell attachment to hydroxyapatite-coated implant surfaces *in vitro*. J Oral Maxillofac Implants. 14:239-47.

Chehroudi B, Ratkay J, Brunette DM. (1992). The role of implant surface geometry on

mineralization *in vitro* and *in vivo*: a transmission and electronmicroscopic study. Cells Mater. 2:89-104.

Chong KH, Chai J. (2003) Strength and mode of failure of unidirectional and bidirectional glass fiber-reinforced composite materials. Int J Prosthodont. 16: 161-6.

Chrisman OD, Snook GA. (1968) The problem of refracture of the tibia. Clin Orthop Relat Res. 60:217-9.

Chung K, Lin T, Wang F. (1998) Flexural strength of a provisional resin material with fiber addition. J Oral Rehabil. 25: 214-7.

Cochran DL, Schenk RK, Lussi A, Higginbottom FL, Buser D. (1998) Bone response to unloaded and loaded titanium implants with a sandblasted and acid-etched surface: a histometric study in the canine mandible. J Biomed Mater Res. 40:1-11.

Cooper LF, Masuda T, Yliheikkilä PK, Felton DA. (1998). Generalizations regarding the process and phenomenon of osseointegration, part 2: *in vitro* studies. J Oral Maxillofac Implants. 13:163-74.

Cordioli G, Mazzocco C, Schepers E, Brugnolo E, Majzoub Z. (2001) Maxillary sinus floor augmentation using bioactive glass granules and autogenous bone with simultaneous implant placement. Clinical and histological findings. Clin Oral Implants Res. 12:270-8.

Davies JE. (1998) Mechanisms of endosseous integration. Int J Prosthodont. 11:391-401.

Davies JE. (2000) Bone formation and healing. In: Bone Engineering. Toronto: em squared Inc. 1–19.

Drouin JM, Cales B. (1994) Yttria-stabilized zirconia for improved hip joint head. In: Andersson ÖH, Yli-Urpo A, editors. Bioceramics 7. London: Butterworth-Heinemann. 387-94.

Duncan JP, Freilich MA, Latvis CJ. (2000) Fiber-reinforced composite framework for implant-supported overdentures. J Prosthet Dent. 84: 200-4.

Evans SL, Hunt CM, Ahuja S. (2002) Bone cement or bone substitute augmentation of pedicle screws improves pullout strength in posterior spinal fixation. J Mater Sci-Mater Med. 13: 1143-5.

Freilich MA, Duncan JP, Alarcon EK, Eckrote KA. (2002) The design and fabrication of fiber-reinforced implant prostheses. J Prosthet Dent. 88: 449-54.

Goldberg AJ, Burstone CJ. (1992) The use of continuous fiber reinforcement in dentistry. Dent Mater. 8:197-202.

Grandini S, Goracci C, Monticelli F, Tay FR, Ferrari M. (2005) Fatigue resistance and structural characteristics of fiber posts: three-point bending test and SEM evaluation. Dent Mater. 2:75-82.

Heimke G. (1990). Aluminum oxide. In: Concise encyclopedia of medical & dental devices. Williams D, editors. Oxford: Pergamon Press. 28-34.

Hench LL. Bioactive glasses and glass-ceramics. (1999) In: Shackelford JF, editor. Bioceramics. Zurich-Uetikon: Transtec Publications Ltd. 37-63.

Hench LL, JK West JK. (1996) In Life Chemistry Reports (Amsterdam, The Netherlands, Harwood Academic Publishers). 178.

Hench LL, Xynos ID, Polak JM. **(2004)** Bioactive glasses for in situ tissue regeneration. J Biomater Sci Polym Ed. 15:543-62.

Hiermer T, Schmitt-Thomas KH, Yang Z. (1998) Mechanical properties and failure behavior of cylindrical CFRP-implant-rods under torsion. Composites. 29: 1453-61.

Huiskes R, Weinans H, Grootenboer HJ, Dalstra M, Fudala B, Slooff TJ. (1987) Adaptive bone-remodeling theory applied to prosthetic-design analysis. J Biomech. 20:1135-50.

Ichikawa Y, Akagawa Y, Nikai H, Tsuru H. (1992) Tissue compatibility and stability of a new zirconia ceramic in vivo. J Prosthet Dent. 68: 322–26.

Isidor F. (1996) Loss of osseointegration caused by occlusal load of oral implants. A clinical and radiographic study in monkeys. Clin Oral Implants Res. 7:143-52.

Isidor F. (1997) Histological evaluation of peri-implant bone at implants subjected to occlusal overload or plaque accumulation. Clin Oral Implants Res. 8:1-9.

Jacobs JJ, Skipor AK, Patterson LM, Hallab NJ, Paprosky WG, Black J, Galante JO. (1998) Metal release in patients who have had a primary total hip arthroplasty. A prospective, controlled, longitudinal study. J Bone Joint Surg Am. 80:1447-58.

Jansen JA, Wolke JG, Swann S, Van der Waerden JP, de Groot K. (1993) Application of magnetron sputtering for producing ceramic coatings on

implant materials. Clin Oral Implants Res. 4:28-34.

Jarcho M. (1992) Retrospective analysis of hydroxyapatite development for oral implant applications. Dent Clin North Am. 36:19-26.

Jemt T, Lekholm U. (1993) Oral Implant treatment in posterior partially edentulous jaws: a 5-year follow-up report. Int J Oral Maxillofac Implants. 8:635-40.

Jemt T, Linden B, Lekholm U. (1992) Failures and complications in 127 consecutively placed fixed partial prostheses supported by Branemark implants. Int J Oral Maxillofac Implants. 7: 40-4.

Klein CP, Wolke JG, de Blieck-Hogervorst JM, de Groot K. (1994) Calcium phosphate plasma-sprayed coatings and their stability: an *in vivo* study. J Biomed Mater Res. 28:909-17.

Kohal RJ, Klaus G, Strub JR. (2006) Zirconia-implant-supported all-ceramic crowns withstand long-term load: a pilot investigation. Clin Oral Implants Res. 17:565-71.

Krauser JT, Boner C, Boner N. (1990) Hydroxyapatite coated dental implants. Biological criteria and prosthetic possibilities. Cah Prothese. 71:56-75.

Kurtz SM, Devine JN. (2007) PEEK Biomaterials in Trauma, Orthopedic, and Spinal Implants. Biomaterials. 28: 4845-69.

Lassila LV, Nohrstrom T, Vallittu PK. (2002) The influence of short-term water storage on the flexural properties of unidirectional glass fiber-reinforced composites. Biomaterials. 23:2221-9.

Lassila LV, Tanner J, Le Bell AM, Narva K, Vallittu PK. (2004) Flexural properties of fiber reinforced root canal posts. Dent Mater. 20:29-36.

Laurell L. (1985) Occlusal forces and chewing ability in dentitions with cross-arch bridges. Swed Dent J Suppl. 26: 160-7.

Leckholm U, Zarb GA. (1985) Patient selection and preparation. In: Branemark P-I, Zarb GA, Albrektsson T, editors. Tissue integrated prostheses: osseointegration in clinical dentistry. Chicago: Quintessence. 199-210.

Lewis G. (2000) Hydroxyapatite-coated bioalloy surfaces: current status and future challenges. Bio-Med Mater Eng. 10:157–88.

Loza-Herrer MA, Rueggeberg FA. (1998) Time temperature profiles of post-cure composite oven. Gen Dent. 46: 79-83.

Loza-Herrero MA, Rueggeberg FA, Caughman WF, Schuster GS, Lefebvre CA, Gardner FM. (1998) Effect of heating delay on conversion and strength of a post-cured resin composite. J Dent Res. 77: 426-31.

Lum LB, Osier JF. (1992) Load transfer from endosteal implants to supporting bone: an analysis using statics. Part two: Axial loading. J Oral Implantol. 18:349-53.

Malaval L, Modrowski D, Gupta AK, Aubin JE. (1994) Cellular expression of bone-related proteins during in vitro osteogenesis in rat bone marrow stromal cell cultures. J Cell Physiol. 158:555-72.

Mao JJ, Major PW, Osborn JW. (1996) Coupling electrical and mechanical outputs of human jaw muscles undertaking multidirectional bite-force tasks. Arch Oral Biol. 41:1141-7.

Mattila R, Puska M, L. Lassila L, Vallittu PK. (2006) Fiber-reinforced composite implant: in vitro mechanical interlocking with bone model material and residual monomer analysis. J Mater Sci: Mater Med. 41:4321-26.

Maxian SH, Zawadsky JP, Durin MG. (1993). Mechanical and histological evaluation of amorphous calcium phosphate and poorly crystallized hydroxylapatite coatings on titanium implants. J Biomed Mater Res. 27:717-27.

Meyer U, Joos U, Mythili J, Stamm T, Hohoff A, Fillies T, Stratmann U, Wiesmann HP. (2004) Ultrastructural characterization of the implant/bone interface of immediately loaded dental implants. Biomaterials. 25:1959-67.

Miettinen VM, Vallittu PK. (1997) Water sorption and solubility of glass fiber-reinforced denture polymethyl methacrylate resin. J Prosthet Dent. 77:531-4.

Mishra AK, Davidson JA, Poggie RA, Kovaac P, Fitzgerald TJ. (1996) Mechanical and tribological properties of diffusion hardened Ti-13Nb-13Zr-A new titanium alloy for surgical implants. In: Mechanical applications of titanium and its alloys: the mechanical and biological issue. Brown S, Lemons J, editors. West Conshohocken, PA: American Society for Testing and Materials. 96-112.

Miyata T, Kobayashi Y, Araki H, Ohto T, Shin K. (2000) The influence of controlled occlusal overload on peri-implant tissue. Part 3: A histologic study in monkeys. Int J Oral Maxillofac Implants. 15:425-31.

Miyata T, Kobayashi Y, Araki H, Ohto T, Shin K. (2002) The influence of controlled occlusal overload on peri-implant tissue. Part 4: a

histologic study in monkeys. Int J Oral Maxillofac Implants. 17:384-90.

Morgan MJ, James DF. (1995) Force and moment distributions among osseointegrated dental implant. J Biomechanics. 28: 1103-9.

Moritz N, Rossi S, Vedel E, Tirri T, Ylanen H, Aro H, Narhi TO. (2004) Implants coated with bioactive glass by CO2-laser, an *in vivo* study. J Mater Sci-Mater Med. 15:795-802.

Naert I, Quirynen M, van Steenberghe D, Darius P. (1992) A study of 589 consecutive implants supporting complete fixed prostheses. Part II: Prosthetic aspects. J Prosthet Dent. 68:949-56.

Naumann M, Blankenstein F, Dietrich T. (2005) Survival of glass fiber reinforced composite post restorations after 2 years-an observational clinical study. J Dent. 33:305-12.

Norton MR, Wilson J. (2002) Dental implants placed in extraction sites implanted with bioactive glass: human histology and clinical outcome. Int J Oral Maxillofac Implants. 17:249-57.

O'Brien, William J. (2002) Dental materials and their selection. Quintessence Publishing Co, Inc. 340-80.

Ogiso M, Nakabayashi N, Matsumoto T, Yamamura M, Lee RR. (1996) Adhesive improvement of the mechanical properties of a dense HA-cemented Ti dental implant. J Biomed Mater Res. 30:109-16.

O'Mahony A, Spencer P. (1999) Osseointegrated implant failures. J Ir Dent Assoc. 45:44-51.

Ong JL, Hoppe CA, Cardenas HL, Cavin R, Carnes DL, Sogal A, Raikar GN. **(1998)** Osteoblast precursor cell activity on HA surfaces of different treatments. J Biomed Mater Res. 39:176-83.

Palussière J, Berge J, Gangi A, Cotten A, Pasco A, Bertagnoli R, Jaksche H, Carpeggiani P, Deramond H. (2005) Clinical results of an open prospective study of a bis-GMA composite in percutaneous vertebral augmentation. Eur Spine J. 14:982-91.

Paphangkorakit J, Osbom JW. (1997) The effect of pressure on maximum incisal bite force in man. Arch Oral Biol. 42: 11–7.

Parr GR, Gardner LK, Toth RW. (1985) Titanium: the mystery metal of implant dentistry. Dental materials aspects. J Prosthet Dent. 54:410-4.

Pastila P, Lassila LV, Jokinen M, Vuorinen J, Vallittu PK, Mantyla T. (2007) Effect of short-term water storage on the elastic properties of some dental restorative materials-A resonant ultrasound spectroscopy study. Dent Mater. 23:878-84.

Piconi C, Burger W, Richter H.G, Cittadini A, Maccauro G, Covacci V, Bruzzese N, Ricci G.A, Marmo E. (1998) Y-TZP ceramics for artificial joint replacements. Biomaterials. 19: 1489-94.

Pilliar RM, Lee JM, Maniatopoulos C. (1986) Observations on the effect of movement on bone ingrowth into porous-surfaced implants. Clin Orthop Relat Res. 208:108-13.

Pjetursson BE, Tan K, Lang NP, Brägger U, Egger M, Zwahlen M. (2004) A systematic review of the survival and complication rates of fixed partial dentures (FPDs) after an observation period of at least 5 years. Clin Oral Implants Res. 15:667-76.

Puleo DA, Nanci A. (1999) Understanding and controlling the bone-implant interface. Biomaterials. 20:2311-21.

Quirynen M, Naert I, van Steenberghe D, Nys L. (1992) A study of 589 consecutive implants supporting complete fixed prostheses. Part I: Periodontal aspects. J Prosthet Dent. 68:655-63.

Radin S, Reilly G, Bhargave G, Leboy PS, Ducheyne P. **(2005)** Osteogenic effects of bioactive glass on bone marrow stromal cells. J Biomed Mater Res A. 73:21-9.

Rangert B, Krogh PH, Langer B, Van Roekel N. (1995) Bending overload and implant fracture. Int J Oralmaxillofac Implants. 10: 326-34.

Richter EJ. (1998) *In vivo* horizontal bending moments on implants. Int J Oral Maxillofac Implants. 13:232-44.

Richter HG, Burger W, Osthues F. (1994) Zirconia for medical implants-the role of strength properties. In: Andersson OH, Yli- Urpo A, editors. Bioceramics 7. London: Butterworth-Heinemann Publ., 401-6.

Rueggeberg FA, Caughman WF, Curtis JW Jr. (1994) Effect of light intensity and exposure duration on cure of resin composite. Oper Dent. 19: 26–32.

Schulte W. (1984) The intra-osseous Al_2O_3 (Frialit) Tuebingen Implant. Developmental status after eight years (I-III). Quintessence International. 15:1-39.

Simon JA, Ricci JL, Di Cesare PE. (1997) Bioresorbable fracture fixation in orthopedics: a comprehensive review. Part I. Basic science and preclinical studies. Am J Orthop. 26:665-71.

Smith DC. (1961) The acrylic denture: mechanical evaluation of midline fracture. Br Dent J. 110: 257-67.

Soballe K, Hansen ES, B-Rasmussen H, Jorgensen PH, Bünger C. (1992) Tissue ingrowth into titanium and hydroxyapatite-coated implants during stable and unstable mechanical conditions. J Orthop Res. 10:285-99.

Stanford CM, Keller JC. (1991) The concept of osseointegration and bone matrix expression. Crit Rev Oral Biol Med. 2:83-101.

Stein GS, Lian JB, Owen TA. (1990) Relationship of cell growth to the regulation of tissue-specific gene expression during osteoblast differentiation. FASEB J. 4:3111-23.

Steinemann SG. (1998) Titanium-the material of choice. Periodontol 2000. 17:7–21.

Sun L, Berndt CC, Gross KA, Kucuk A. (2001) Material fundamentals and clinical performance of plasma-sprayed hydroxyapatite coatings: a review. J Biomed Mater Res Appl Biomater. 58:570-92.

Tanner J, Robinson C, Soderling E, Vallittu PK. (2005) Early plaque formation on fiber-reinforced composites *in vivo*. Clin Oral Investig. 9: 154-60.

Tanner J, Vallittu PK, Soderling E. (2001) Effect of water storage of E-glass fiber-reinforced composite on adhesion of Streptococcus mutans. Biomaterials. 22: 1613–8.

Tuusa SM, Lassila LV, Matinlinna JP, Peltola MJ, Vallittu PK. (2005) Initial adhesion of glass fiber-reinforced composite to the surface of porcine calvarial bone. J Biomed Mater Res B Appl Biomater. 75:334–42.

Tuusa SM, Peltola MJ, Tirri T, Lassila LV, Vallittu PK. (2007) Frontal bone defect repair with experimental glass-fiber-reinforced composite with bioactive glass granule coating. J Biomed Mater Res B Appl Biomater. 82:149-55.

Tuusa SM, Peltola MJ, Tirri T, Puska MA, Röyttä M, Aho H, Sandholm J, Lassila LV, Vallittu PK. (2008) Reconstruction of critical size calvarial bone defects in rabbits with glass-fiber-reinforced composite with bioactive glass granule coating. J Biomed Mater Res B Appl Biomater. 84:510-9.

Vallittu PK. (1998) Some aspects of the tensile strength of unidirectional glass fiber-polymethymethacrylate composite used in dentures. J Oral Rehabil. 25: 100-5.

Vallittu PK. (1995) The effect of void space and polymerization time on transverse strength of acrylic-glass fiber composite. J Oral Rehabil. 22: 257-61.

Vallittu PK. (2007) Effect of 10 years of in vitro aging on the flexural properties of fiber-reinforced resin composites. Int J Prosthodont. 20:43-5.

Van Eijden TM. (1991) Three-dimensional analyses of human bite-force magnitude and moment. Arch Oral Biol. 36: 535-9.

Van Mullem PJ, de Wijn JR. (1988) Bone and soft connective tissue response to porous acrylic implants. A histokinetic study. J Craniomaxillofac Surg. 16:99-109.

Van Noort R. (2002) Mechanical properties. In: van Noort R, editor. Introduction to dental materials. Edinburgh: Mosby. 42-49.

Van Steenberghe D, Naert I, Jacobs R, Quirynen M. (1999) Influence of inflammatory reactions vs. occlusal loading on peri-implant marginal bone level. Adv Dent Res. 13:130-5.

Vidyasagar L, Apse P. (2003) Biological response to dental implant loading/overloading. Implant overloading: Empiricism or science. Stomatologija, Baltic Dental and Maxillofacial Journal. 5: 83-9.

Weinberg LA. (1993) The biomechanics of force distribution in implant-supported prostheses. Int J Oral Maxillofac Implants. 8: 19-31.

Wennerberg A, Albrektsson T, Johansson C, Andersson B. **(1996)** Experimental study of turned and grit-blasted screw-shaped implants with special emphasis on effects of blasting material and surface topography. Biomaterials. 17:15-22.

Wolff J. (1986) The law of bone remodeling/ translated by Maquet PGJ and Furlong R. New York: Springer-Verlag.

Yao J, Radin S, Reilly G, Leboy PS, Ducheyne P. (2005) Solution-mediated effect of bioactive glass in poly (lactic-co-glycolic acid)-bioactive glass composites on osteogenesis of marrow stromal cells. J Biomed Mater Res A. 75:794-801.

Yuehuei H. (2000). ‘‘Mechanical properties of Bone. Mechanical Testing of Bone and the bone-Implant Interface’’. CRC Press.43.